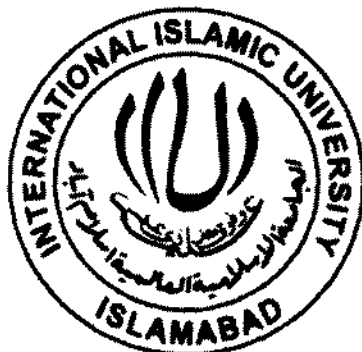


**Structural and Electrical Properties of Copper doped  
SnSbS Thin film.**



**By:**

**Sabir Khan.**

(140-FBAS/MSPHY/F12)

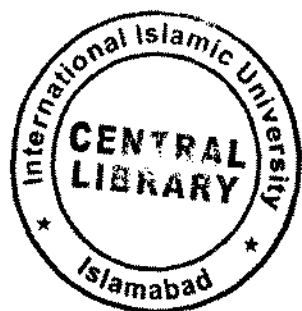
**Supervisor:**

**Dr. Waqar Adil Syed.**

Associate Professor

Department of Physics, FBAS, IIUI

**Department of Physics  
Faculty of Basic and Applied Sciences  
International Islamic University, Islamabad**



(2015)

ii



Accession No TH-14549 (K) 9/10

\*

MS  
620.182  
SAS

Copper  
Material science  
Magnetic spurling  
Solar cell.



**INTERNATIONAL ISLAMIC UNIVERSITY, ISLAMABAD  
FACULTY OF BASIC AND APPLIED SCIENCES  
DEPARTMENT OF PHYSICS**

**Final Approval**

It is certified that the work presented in the thesis entitled “**Structural and Electrical Properties of Copper doped SnSbS Thin Film**” by **Sabir Khan** bearing **Registration No. 140-FBAS/MSPHYY/F12** is of sufficient standard in scope and quality for award of degree of MS Physics from International Islamic University, Islamabad.

**COMMITTEE**

**External Examiner**

  
.....

**Internal Examiner**

  
.....

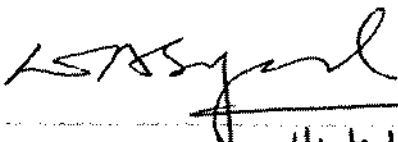
Department of Physics, FBAS, IIUI

**Supervisor:**

Dr. WaqarAdil Syed

Associate Professor and Chairman

Department of Physics, FBAS, IIUI

  
.....  
14.4.15

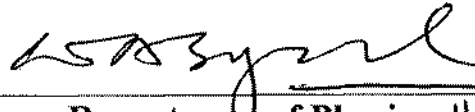
# **Structural and Electrical Properties of Copper doped SnSbS thin film.**

**By:**

**Sabir Khan.**

**(140-FBAS/MSPHY/F12)**

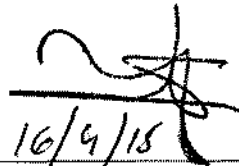
This Thesis submitted to Department of Physics International Islamic University, Islamabad  
for the award of degree of MS Physics



**Chairman Department of Physics 14-4-15**

**CHAIRMAN  
DEPT. OF PHYSICS  
International Islamic University  
Islamabad**

**International Islamic University Islamabad**



**16/4/15**

**Dean Faculty of Basic and Applied Science**

**International Islamic University, Islamabad**

# *DEDICATED*

*To*

*My Loving Parents*

*Brothers*

*and*

*Respected Teachers.*

## Declaration

I **Sabir Khan** (Registration no # 140-FBAS/MSPHY/F12), student of MS Physics (session 2012-2014), hereby declare that the matter presented in the thesis titled “Structural and Electrical Properties of Copper doped SnSbS thin film” is my own work and has not been published or submitted as research work or thesis in any form in any other university or institute in Pakistan or abroad.

**Sabir Khan.**

(140-FBAS/MSPHY/F-12)

Signature----------

Dated: 14/04/2015

## Forwarding Sheet by Research Supervisor

The thesis entitled “**Structural and Electrical Properties of Copper doped SnSbS thin film**” submitted by **Sabir Khan** (Registration no # 140-FBAS/MSPHY/F12) in partial fulfillment of MS degree in Physics has been completed under my guidance and supervision. I am satisfied with the quality of his research work and allow him to submit this thesis for further process for MS degree from Department of Physics, as per IIU Islamabad rules and regulations.

Dated: \_\_\_\_\_

**Dr. Waqar Adil Syed,**  
Associate Professor  
Department of Physics,  
International Islamic University,  
Islamabad.



## Acknowledgment

My foremost acknowledgement is to that unseen power who governs all the affairs of nature and mans the all mighty Allah, because it was due to the blessing of him that I could complete my research work successfully. At the same time, I offer my humble words of thanks and gratitude to the towering personality of the Holly Prophet (PBUH) fountain of light, guidance and knowledge to all human beings.

Second to Allah and his prophet (PBUH) I consider the personality of my reverend and eminent supervisor **Dr. Waqar Adil Syed** to be a great source of inspiration for me I acknowledge his pivotal contribution in the form of skillful suggestions and keen interest which he showed in my work.

Thirdly, once again I am thankful to my Chairman **Dr. Waqar Adil Syed** and I acknowledge his contributions in my research work by guides me and facilitated my work in the library of my department.

Fourthly I m grateful to Dr Yaqoob khan, Dr Ishaq and Mr Turab of NCP for their full co-operation. They provided me the facilities of XRD, UV, DRS and RBS.

Many thanks to Dr Iftekhar Gul of NUST to provid me the Hall Measurement effect. Finally I acknowledge the power of the sincere prayers and good wishes of my parents , my brothers , my teachers , my friends and all the nears dears which led me to the path of success in my research work.

**Sabir Khan.**

Dated- 14/04/2015

## Contents

### CHAPTER 1 Introduction

1.1 Thin film .....	1
1.2 Uses of thin film.....	2
1.3 Solar or photovoltaic cell(PV).....	2
1.4 Material for solar cell.....	4
1.5 Thin film and grain size.....	5
1.6 preparation of sample.....	5
1.7 Effect on the properties of SnSbS doped by copper.....	5
1.8 Literature review.....	6

### CHAPTER 2 Sample preparation and deposition techniques.

2.1 Sample syntheses.....	8
2.2 Sample preparation.....	8
2.3 Deposition techniques.....	8
2.3.1 Physical Vapor Deposition Techniques (PVD).....	8
2.3.1.1 Electron Beam Evaporation.....	9
2.3.1.2 Thermal Vacuum Evaporation.....	10
2.3.1.3 Magnetic spurling .....	11
2.3.1.4 Molecular Beam Epitaxy (MBE).....	12
2.4 Chemical Vapor Deposition.....	13

### CHAPTER 3 Characterization techniques

3.1 Characterization techniques.....	15
3.1.1 X- ray diffraction (XRD).....	15
3.1.2 Spectroscopy.....	16
3.1.3 Fourier transformation infra red spectroscopy (FTIR).....	17

3.1.4 Rutherford backscattering spectroscopy (RBS) .....	19
3.1.5 Hall measurement effect.....	23
3.1.6 UV Visible Spectroscopy.....	24
3.1.7 Defuse reflectance spectroscopy(DRS).....	26
CHAPTER 4 Experimental setup and work	
4.1 Vacuum thermal evaporation .....	28
4.2 Material used for the sample preparation .....	29
4.3 Substrate selection.....	29
4.4 Substrate cleaning .....	30
4.5 Preparation of Tin antimony sulfide doped by copper thin film.....	31
CHAPTER 5 Result and discussions	
5.1 Rutherford backscattering spectroscopy. ....	32
5.1.1 Thickness and composition of elements in films.....	34
5.2 The Hall Effect Measurements .....	35
5.3 Structural property.....	40
5.3.1 Indexing.....	40
5.3.2 Calculation of grain size .....	41
5.3.3 Inter planer distance “d”.....	42
5.3.4 Micro strain.....	42
5.3.5 Dislocation density.....	42
5.4 Optical characterization.....	44
Conclusion.....	52
References.....	53

## Figures Captions

<b>Figure 1.1:</b> Structure of C-Si photovoltaic cell .....	2
<b>Figure 1.2:</b> PV-system .....	4
<b>Figure 2.1</b> Schematic diagram of electron beam evaporation.....	10
<b>Figure 2.2:</b> Schematic diagram of thermal vacuum evaporation.....	11
<b>Figure 2.3:</b> Schematic diagram of MBE .....	13
<b>Figure 3.1:</b> Schematic diagram of Bragg's Diffraction law.....	16
<b>Figure 3.2:</b> Schematic diagram of spectrometer .....	17
<b>Figure 3.3:</b> Schematic diagram of zero path difference of interferometer .....	18
<b>Figure 3.4:</b> Schematic diagram of Michelson interferometer .....	19
<b>Figure 3.5:</b> Schematic diagram of Rutherford back scattering .....	20
<b>Figure 3.6:</b> Schematic diagram of scattering Analyzing techniques .....	21
<b>Figure 3.7:</b> Schematic diagram of Hall Effect .....	24
<b>Figure 3.8:</b> Schematic diagram of UV visible spectrometer.....	26
<b>Figure 3.9:</b> Schematic diagram of Defuse reflection .....	26
<b>Figure 4.1:</b> Schematic diagram of vacuum thermal evaporation.....	28
<b>Figure 5.1:</b> Graph of Channel/Energy and Normalize Yield of sample 1.....	33
<b>Figure 5.2:</b> RBS graph of simulated and experimental.....	33
<b>Figure 5.3:</b> Comparison RBS spectra of all samples .....	34
<b>Figure 5.4 and 5.5:</b> Resistivity and thickness graph.....	38
<b>Figure 5.6 and 5.7:</b> Conductivity and thickness graph.....	39
<b>Figure 5.8 and 5.9:</b> Mobility and thickness graph.....	39
<b>Figure 5.10 and 5.11:</b> XRD pattern of sample i and ii.....	40
<b>Figure 5.12 and 5.13:</b> XRD pattern of sample iii and iv.....	41
<b>Figure 5.14:</b> XRD pattern of all samples (i,ii.iii.iv).....	41
<b>Figure 5.15:</b> Copper concentration and Diameter (Percentage) .....	43
<b>Figure 5.16:</b> Copper concentration and dislocation densities.....	43
<b>Figure 5.17:</b> Graph of as deposited Transmission of all sample.....	44

**Figure 5.18:** Graph shows maxima and minima of Transmission and Wavelength .....45

**Figure 5.19:** Transmission spectra after doping.....46

**Figure 5.20:** Reflection spectra after doping (240nm).....47

**Figure 5.21:** Reflection spectra after doping (690nm).....47

**Figure 5.22:** Reflection spectra after doping (730nm).....48

**Figure 5.23:** Graph without doping..... 49

**Figure 5.24 and 5.25:** Energy band gap graph of sample 1and 2 after doping.....50

**Figure 5.26:** Energy band gap graph of sample 3 after doping.....50

**Figure 5.27:** Copper concentration and band energy graph.....51

### List of Tables

<b>Table 5.1</b>	Thickness and elemental composition.....	35
<b>Table 5.2</b>	Hall's measurements of sample 1.....	37
<b>Table 5.3</b>	Hall's measurements of sample 2.....	37
<b>Table 5.4</b>	Hall's measurements of sample 3.....	38
<b>Table 5.5</b>	Optical properties of annealed samples.....	42
<b>Table 5.6</b>	Copper concentrations and refractive index.....	46
<b>Table 5.7</b>	Concentration and binding energy.....	49

### List of abbreviations

<b>Sn:</b>	Tin
<b>Sb:</b>	Antimony
<b>S:</b>	Sulfur
<b>Cu:</b>	Copper
<b>RBS:</b>	Rutherford back scattering spectroscopy
<b>XRD:</b>	X-ray diffraction
<b>PVD:</b>	Physical vapor deposition
<b>CVD:</b>	Chemical vapor deposition
<b>MBE:</b>	Molecular beam epitaxy
<b>PV:</b>	Photovoltaic
<b>IR:</b>	Infra red
<b>DRIFT:</b>	Diffuse reflectance infra red Fourier transformation
<b>UV:</b>	Ultra violet
<b>DRS:</b>	Diffuse reflectance spectroscopy
<b>c-si</b>	Crystalline silicon
<b>a-Si</b>	Amorphous silicon

## Abstract

Tin antimony sulfide thin film was deposited on glass substrate by two source thermal evaporation methods. The as-deposited thin film exhibits amorphous structure. Copper was doped by simply dipping the samples into the copper nitrate solution for 20 minutes. The films were dried and annealed for 25 minutes at a temperature 150°C. The structural, optical and electrical characteristics were determined by X-ray diffraction, Rutherford backscattering, UV Visible spectroscopy and Hall effect measurements. From the XRD analysis it was confirmed that the thin films were orthorhombic with a preferred orientation along in the (320) plane. The grain size was found increasing with the increasing concentration while the dislocation densities, refractive index and micro strains of the films were decreased. The band gap energy of the films were calculated from the optical spectroscopy was decreased with increasing thickness and copper concentration. The binding energy of the films were decreased from 1.62 to 1.49 eV. Electrical properties of the films were studied by Hall effect measurement system, which reveals that due to doping the resistivity of the films were decreased while conductivity and mobility of the films increased. The work has been carried out to look the suitable and efficient material for solar cell application which are abundant, cheap and environment friendly.



# Chapter # 1

## Introduction

### 1.1 Thin film.

Thin film is a layer of material with thickness in a range from a few nanometers to some of micrometers. It is deposited over a clean and clear substrate like glass or wafer. Portmans and Arkhipov [1] define thin films as “that can be obtained over clean and clear glass substrate by growth and nucleation process”. According to them the properties like chemical, physical and structural totally depend upon the thickness and grain size of thin films.

Harsha [2] stated that thin films are used in decorative parts, electronic devices and for the development of new nano size materials. The thin films of ferroelectric and ferromagnetic [3] materials are used as a memory devices of computer.

Thin films have a lot of application in different fields of daily life. These are used in batteries, in solar cells, in research of inorganic oxides films, for the syntheses of transparent transistors which are less expensive and can be used for the commercial purposes easily, which are stable and environment friendly. [4].

Baran [5] showed that a quick change in thin films devices and nano material developed a new technology and materials. He also showed the need and importance of research activity for the improved knowledge and best productivity capabilities for the chemical and physical properties of micro structures and also for the application of thin films into various potentials.

The deposition techniques are mainly of two types whether it is chemically or physically. In the first one, that is in a precursor of the form of liquid goes to the process of chemical changes and deposited at the surface of glass/solid substrate and formed a solid thin film. While in physical deposition techniques the thin film of solid is produced by mechanical, electromechanical or thermodynamic way [6].

### 1.2 Uses of thin film.

Thin films are used almost in each field of modern physics. But the most common uses of thin films are in:

1. Electronic devices.

2. Semiconductor devices.
3. Optical coating.
4. Solar cells.
5. House hold mirror.
6. Computer memory chip.
7. Pharmaceutical uses.

### 1.3 Solar cell or photovoltaic (PV) cell.

Due to decline in the available energy resources and their increasing demand [7-10] it is the dire need of the day to find out new and cheap resources of energy. The researchers try to overcome difficulties in the field of energy by discovering new ways and devices. Solar cell or PV cell [8, 11] is one of the most suitable discovery. A solar cell is an electric instrument which convert light energy i.e. photons in to electric current (electrical energy). For the working of solar cell we usually need the following.

1. The absorption of photons to emit excitons.
2. The detachment of charge carriers of opposite sign (+ive and -ive).
3. The moving of these charges to respective terminal in the external circuit.

The C-Si photovoltaic cells with complete parts are shown in Figure 1.1.

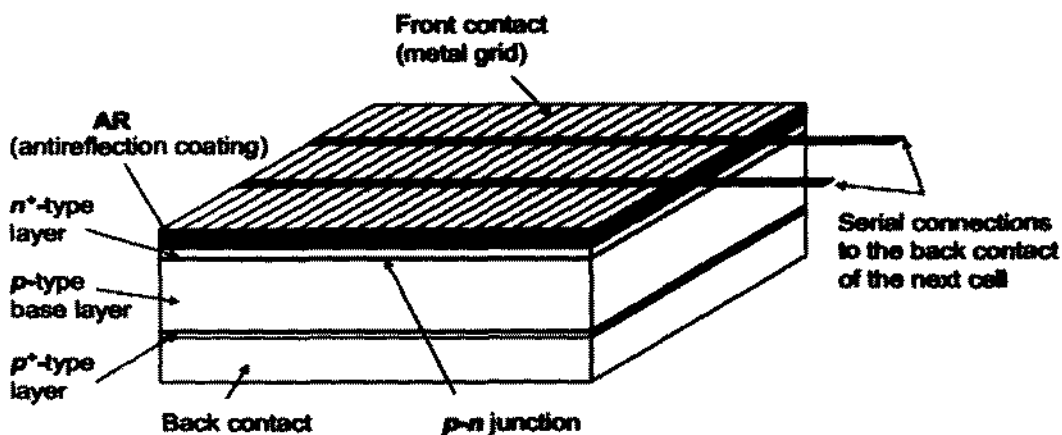


Figure 1.1 Structure of C-Si Photovoltaic cell.

A number of solar cells combine and form a solar module, solar modules combine and form solar panel, solar panels are combined to form solar array, so in this way a PV system is formed which produces electrical energy from solar energy. The complete diagram of the PV system is shown in figure 1.2. The first working solar cell was introduced by Calvin Souther Fuller and Gerald Pearson [12] at Bell Laboratories [13].

Solar cell can be classified into three (03) generations.

- i. The first generation of photovoltaic cells is called wafer or slice or substrate [14].
- ii. The 2<sup>nd</sup> generation of photovoltaic cell is called thin film. Which are A-Si, cadmium telluride (CdTe), SbS etc. Most of the film panels have less percentage of efficiency i.e. 2 to 3 than C-Si solar cell [15].
- iii. The third generation of solar cell contains multilayer semiconductor junction grown one above the other which almost explain as emerging solar cell. Like triple junction photovoltaic cell of gallium arsenide (GaAs), Gallium (Ga) and indium gallium phosphide (InGaP) [16].

## From a solar cell to a PV System

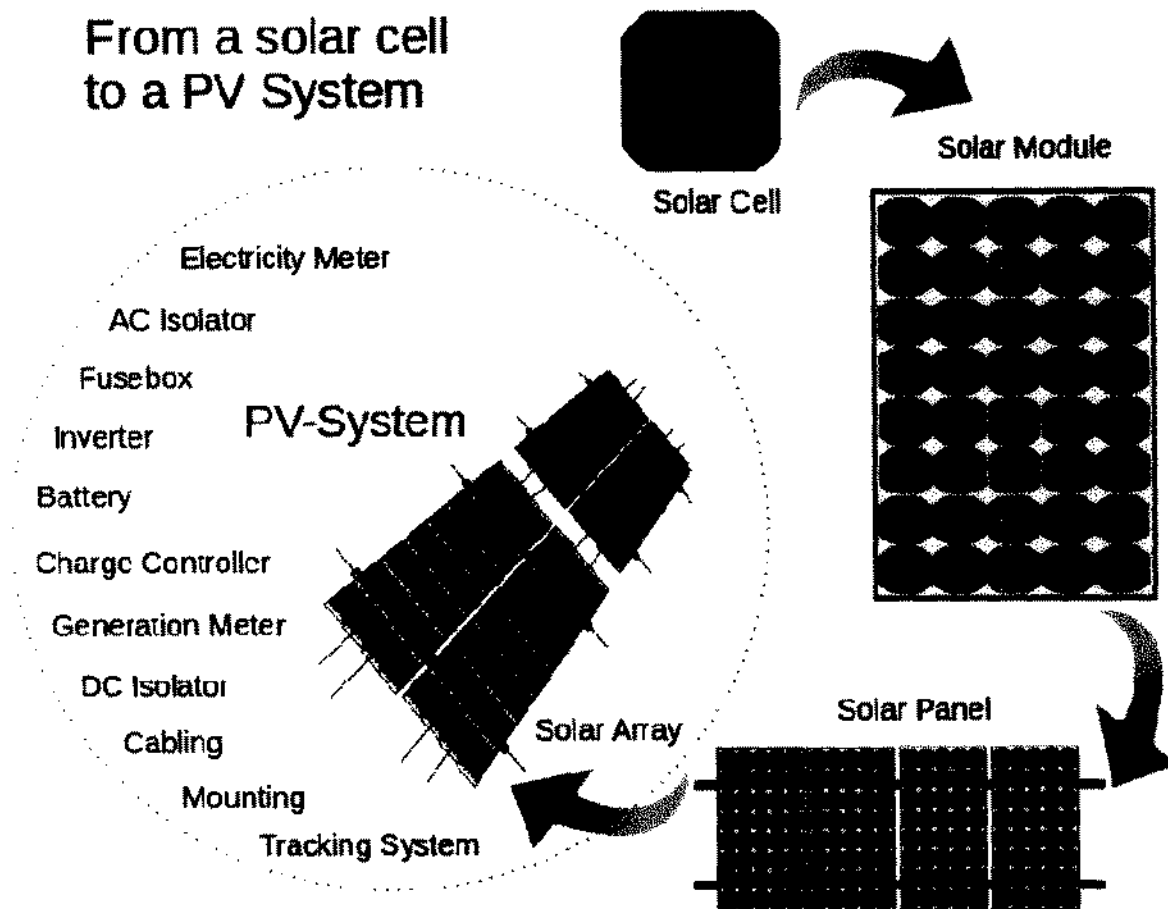


Figure 1.2 PV-System

### 1.4 Materials for solar cell.

The most suitable material for solar cell is silicon (Si), however the processing of silicon to be used in a solar cell is very expensive. A huge number of materials have semiconducting properties [17] including group XIV of the periodic table in which the most effective are silicon (Si) and Germanium (Ge). The binary compounds such as GaAs which belong to third (III) and fifth (V) groups. GaAs is also used in laser diode, infrared LED and optical window [18]. The compounds of groups II and VI, IV and V are also used in solar cells. The II and VI groups are not environment friendly, extremely expensive and highly toxic. Therefore the researchers start to work on such semiconducting materials which are cheaper, non toxic and environment friendly. In recent decade a large number of researcher /scientists are studying the physical

properties of chalcogenides material thin films which have a lot of applications in photovoltaic devices [19, 20].

### **1.5 Thin film and Grain size.**

The one dimension's of a thin film is so small that it changes the properties of the thin film i.e. the properties like optical, structural and electrical changes are due to dimension of thin film. This behavior of the material used is called quantum confinement and it totally depends upon the thickness of the thin film [21].

The gradient of the material shows some extraordinary characteristics due to the confinement in the grain size (dimension). It was also found independently that thin film deposition by thermodynamic compositional process.

According to Rontein F-Bursha [22], that different thin film can be deposited from bulk materials.

### **1.6 Preparation of sample.**

Tin antimony sulfide ( $\text{SnSb}_2\text{S}_3$ ) thin film were deposited on clean glass substrate by vacuum thermal evaporation process at the pressure in range of  $10^{-3}$  to  $10^{-5}$  torr and then the thin film were annealed at 150 degree Celsius. The annealed thin films on glass substrate were of different thicknesses. Then the film was cut into different pieces by the help of diamond cutter. Now dark blue copper nitrate were solved in pure water and all the pieces of film were dipped in the solution for about 15 to 20 minutes. And then the films were taken out of the solution and dried. now the films were annealed in electric furnace at  $150^\circ\text{C}$  for at least 30 minutes and then removed. Now the films are ready for XRD, UV, DRS, RBS, and hall measurement effect for the purpose to know their electrical properties, physical properties and deposition of Copper, Tin, Antimony and Sulfur.

### **1.7 Effects of copper doping on the properties of tin antimony sulfide (SnSbS) thin film.**

Structural characteristics of SnSbS thin film are completely changed as compared to bulk materials, and so their optical electrical, physical properties etc. are also changed. This is due to the change in grain size of the material. When copper is doped to SnSbS thin film then the properties will definitely be changed. The calculated properties of the thin film SnSbS doped by copper are given in chapter no 5.

## 1.8 Literature review.

Pure or doped  $\text{Sb}_2\text{S}_3$  which belongs to  $\text{V}_2 - \text{VI}_3$  groups of semiconductors have a lot of applications in optoelectronic devices, solar cell, thermoelectric cooling devices technology and special type camera design for TV [19, 20],[23,24]. The reason for this is the direct band gap i.e. in range about 1.78-2.5 eV [25,26] and better energy absorption i.e.  $10^5 \text{ cm}^{-1}$ . But despite of this  $\text{Sb}_2\text{S}_3$  have a very high resistivity to minimize or to made it p type or n type semiconductors tin (sn) is doped to it. A thin film of Sn doped  $\text{Sb}_2\text{S}_3$  was deposited on the glass substrate at temperature of  $240^\circ\text{C}$  by thermal evaporation method and then the optical and electrical properties were studied by F.Aousgi and M kanzari.

Sulfosalte thin films have a lot of uses in optoelectronic devices [19, 20], [27- 29]. This is the reason that the researchers use these materials in the solar cell to prepare alternate sources of energy. Among the available sulfosalte  $\text{Sb}_2\text{S}_3$  pure and doped are used in the solar cell, thermoelectric cooling devices and photoconductive target for Videocon TV camera [30,31]. SnS is one of the cheap material which is used in solar cell due its band gape energy of 1.3~1.4eV and a basic absorption coefficient above  $10^5 \text{ mm}^{-1}$ [32] belongs to IV-VI groups(semiconductors compound). When it is highly pure then it is "p" type, but by doping Sb or  $\text{Sb}_2\text{S}_3$  it becomes "n" type semiconductor compound. The physical and electrical properties of " SnS" shows that this compound has the great potential in photovoltaic application by using II-VI groups as a window layers in similar devices like CdTe, CIS, it is more important that the constituents of these compounds are available easily and also non toxic to the environment. Antimony Sulfide thin films can be grown in a number of methods i.e. Solgel methods [32], Chemical methods [32, 34] and Vacuum thermal evaporation techniques.

As this is dire need of the day that new resources of energy and fuel be explored by cheapest and non toxic way, in which the most favorable is the photovoltaic devices [8,10,11][36,38]. New compounds with good physical and electrical properties [11, 40] are always needed, that is why the researchers started to work on same project. Amorphous Si, C-Si, CdTe and CIGS are already in using in solar cell. But these compounds have one or other disadvantages, i.e. C-Si is very high efficient but very expensive and indirect band gape, Cd is toxic and is very rare [39, 40]. So a sulfosalte type chalcogenides film has become the focus of the researchers for the reason of direct band and large coefficient of absorption. These are less toxic, easily available, abundant and good absorber layer to the light, due to these reasons the searchers think to study

the physical, electrical properties and surfaces for the manufacturing of photovoltaic cell technology [41, 42].

Many minerals type sulfide are grouped in to semiconductors [43]. The basic properties of the semiconductors type minerals are the band energy i.e. the gap between valance band and empty conduction band. The bonding of minerals like ternary sulfide is very complicated [44]. The optical pumping of the electrons in semiconductors type materials in the band gap is strongly allowed. Which is called optical absorption edge. The optical absorption edge for the materials whose band gap energy is in range from 0.5 to 3 eV can be easily calculated by using optical spectroscopy, however for the filled band state the optical absorption edge has a lowest energy absorption, which included the states spanning 30 to 50 eV energy [45].

## Chapter # 2

### Sample preparation and deposition techniques

#### 2.1 Sample Synthesis.

For the syntheses of Tin doped Antimony sulfide (SnSbS), SnS and Sb<sub>2</sub>S<sub>3</sub> were the starting materials. SnS was prepared from Sn and S powder according to scheme in reference [46] in ratio 0.7873g and 0.2127g simultaneously. Both the powders were grind to mix completely, placed in a vacuum tube in presence of Argon gas, Annealed at 600 °C for 24 hours and allowed to cool slowly to form SnS. A highly pure 99.9% Sb<sub>2</sub>S<sub>3</sub> were purchased from the market (Sigma Aldrich).

**2.2 Sample preparation.** Both the powders i.e. (SnS and Sb<sub>2</sub>S<sub>3</sub>) were evaporated in a vacuum thermal evaporator chamber by two sources method (most suitable) from the boat of Aluminum Oxide to deposit the film on the substrate. For accurate deposition of thin film on the substrate the evaporation from the source were managed by the base material from the Aluminum Oxide boats. The pressure of the chamber were kept in range of 10<sup>-5</sup> torr without heating substrate. The as deposited thin film was annealed at 125 °C in the presence of argon gas.

#### 2.3 Deposition techniques.

According to Karishna Seshan [47], deposition technologies are the back bone in the manufacturing of microelectronic instruments made through thin film.

Mainly there are two methods which are used for deposition techniques.

1. Physical vapor deposition (PVD)
2. Chemical vapor deposition (CVD)

##### 2.3.1 Physical Vapor Deposition techniques (PVD)

It is that type of method in which a material is evaporated to form a gaseous beam which is then condensed in the form of layer or film over a clean substrate like glass etc. (substrate used is mostly glass because it is easily available in the market and cheap).



Physical vapor deposition is further divided into various techniques, which are given below.

- ❖ Electron beam evaporation.
- ❖ Thermal evaporation.
- ❖ Magnetic sputtering.
- ❖ Pulse filtered cathode arc deposition.
- ❖ RF sputtering.
- ❖ Molecular beam epitaxial.
- ❖ Evaporative deposition.

### **2.3.1.1 Electron Beam Evaporation.**

This type of evaporation techniques is used in industrial application, in which base material is evaporated with the help of highly energetic electron beam bombarded from electron gun. By the help of this technology one can generate a very quick deposition rate up to 25000 Å/min. a highly energetic beam of electron from the electron gun is focused with the help of magnetic and electric field. With the help of these energetic electrons a huge amount of energy is generated, which further evaporates the base material placed in the crucible. The whole system is attached with the highly vacuum pump to avoid any type of chemical reaction with gases on the substrate. As a result vapor of the base material condenses over a substrate placed just above the crucible and form thin film [48].

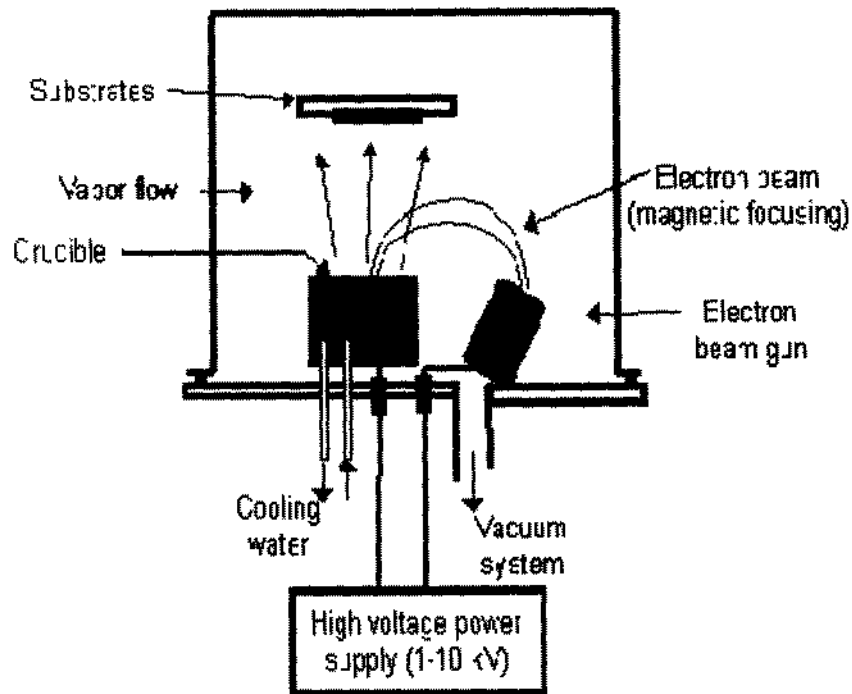


Figure 2.1 Electron Beam Evaporation

### 2.3.1.2 Thermal Vacuum Evaporation Methods.

In this technique base material, in the form of solid or liquid is converted into vapors and deposited over a substrate to form thin film under finite pressure of vapors, the whole system is attached with vacuum pump (The phenomenon is called sublimation, while from liquid to vapor is called evaporation). Typically in this type of physical vapor deposition the source material is placed near a filament, heated crucible when voltage is applied, which is further heated to the source, where the base material is placed and as a result evaporation takes place and condense over a substrate to form a thin film as shown in diagram.

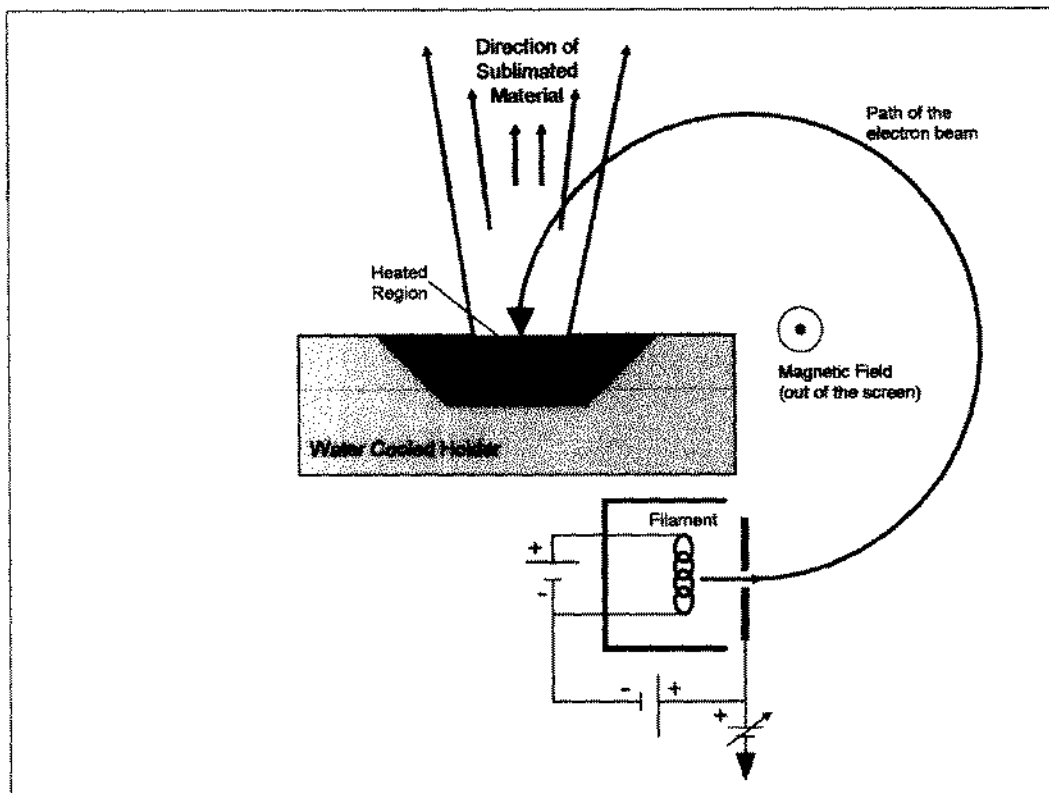


Figure 2.2 Schematic Diagram of Thermal Vacuum Evaporation

This type of deposition technique has some disadvantages i.e. in this technique one cannot evaporate a base material of high melting point [2]. That is why this type of technique is not universally popular. However it has also some advantages i.e. Apparatus and installation cost rate is comparably less expensive, and simple to operate.

### 2.3.1.3 Magnetic Sputtering.

In this type of techniques atoms/molecules are removed from the solid target (base material) by the bombardment of highly energetic electrons. The base material in the substrate is placed over the electron side by side inside a chamber with inert gas. These sputtered atoms/molecules are condensed over a substrate to form a thin film. In this type of techniques the base material is in the form of solid so no need to change the base material into gaseous form and very low energy is radiated through the substrate. There are also other energy methods for sputtering techniques which include ion sputtering RF sputtering, 3D/off axis sputtering, triode sputtering and ion plating [49]

#### **2.3.1.4 Molecular Beam Epitaxy (MBE).**

This type of technique is widely used for the fabrication of semiconductor type devices like transistors; wifi etc. It was invented by J.R. Arther and Alfred [50] in late 1960 in the bell laboratories. This type of deposition techniques require ultra high vacuum in which the thin film is grown epitaxially. This is the combination of two Greek words i.e. epi and taxes which means above and in an order manner), with the deposition rate less than 3000 nm/hour. To measure the thickness of each epitaxial crystal layer during working reflection high energy electron diffraction (RHEED) is used in computerized way. In some cases it is important to keep the substrate at low temperature, and this is achieved with the help of cryo pump. This type of technique is also used for the deposition of some type of organic semi conductor. In this method instead atoms, molecules are evaporated and form a thin film over substrate. This method of deposition becomes complex and time consuming due to ultra high vacuum and low deposition growth rate. Although it is its drawback, but however due to this it provides accurate control over the interfaces [51]. The modified form of MBE [52] is also used for the deposition of materials like oxides for advanced optical, electronic and magnetic applications. The schematic diagram of MBE is shown below.

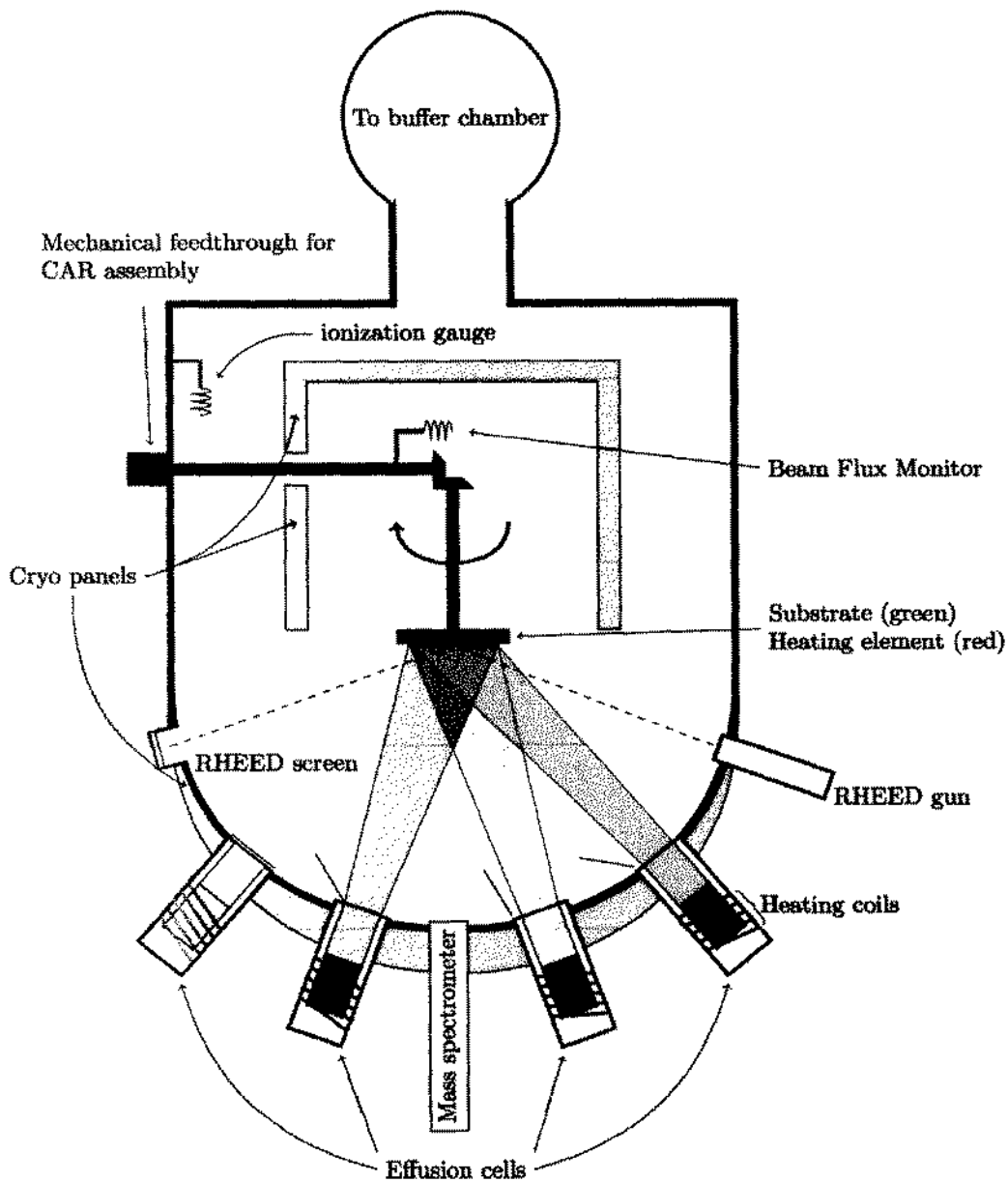


Figure 2.3 Schematic diagram of MBE

## 2.4 Chemical vapor depositions (CVD).

By the help of chemical vapor deposition techniques one can fabricate a highly proficient and pure thin film. This type of method is used for the fabrication of carbon nano tubes [66]. In this deposition the volatile precursor reacts chemically and deposited on the desired substrate, while

the product during the deposition is removed from the chamber in the form of gas flow. It is further divided into different type's i.e.

1. **By operating pressure.** Chemical vapor deposition is divided into:

- ❖ Atmospheric pressure chemical vapor deposition (APCVD).
- ❖ Low pressure chemical vapor deposition [53].
- ❖ Ultra high vacuum chemical vapor-deposition (UHVCVD).

It may be noted that almost all modern/new techniques are either LPCVD or UHVCD.

2. **Chemical vapor deposition by physical characteristic of vapors.**

These are further subdivided into the following types.

- ❖ Aerosol assisted chemical deposition (AACVD).
- ❖ Direct liquid injection chemical vapor deposition (DLICVD).
- ❖ Atomic layer chemical vapor deposition
- ❖ Vapor phase epitaxy (EVPE)
- ❖ Photo initiated chemical vapor deposition (PICVD)
- ❖ Metal organic chemical vapor deposition (MOCVD)
- ❖ Rapid thermal chemical vapor deposition (RTCVD)
- ❖ Hybrid Plasma methods
- ❖ physical chemical vapor deposition (HPCVD)
- ❖ Hot filament chemical vapor deposition (HFCVD)

## CHAPTER # 3

### Characterization techniques.

#### 3.1 Characterization techniques.

To study the physical properties like electrical, optical, magnetic, crystalline structure the following characterization are important.

##### 3.1.1 X-ray diffraction (XRD).

This is an important technique, which is used to investigate structure of the material crystal including imperfections, atomic arrangement and crystallite size. Due to neutral in nature it is very useful for studying the internal layer and also not harmful to the film as well as bulk material. X-rays technique is used to find out the grain size, micro strain, and thin film dislocation energy and along with bulk material stresses.

When the X-ray fall on the material, there occur elastic and inelastic collision between the X-rays and electron, which after scattering give information about the material. Diffraction pattern is produced when X-rays interact with different material crystalline which is diffracted from the plan of crystal. Sharp peaks are produced due to the periodic repetition of atoms due to diffraction pattern. While in case of amorphous material diffraction pattern shows no such sharp peak. However it is observed that each substance shows its own pattern which is different from others [2].

##### Methods used to measure diffraction.

Following are the different methods which are used for the measurement of X-Ray diffraction.

1. Powder diffraction.
2. Small angle X-Rays scattering method (SAXS) range= $0.1^\circ$  to  $10^\circ$
3. Laue diffraction methods.(i Back reflection Laue. ii Transmission Laue).
4. Double crystalline diffraction.

It may be noted that X-Rays diffraction is totally based on Bragg's law. i.e. according to this law,

$$n\lambda = 2d\sin\theta \quad 3.1$$

Where  $n$  is order of diffraction having values 1,2,3,4....., " $\lambda$ " is wavelength of the X-Rays " $d$ " is the inter planner distance, " $\theta$ " is angel between incident ray and scattering ray. All these can easily be understood from the diagram given below.

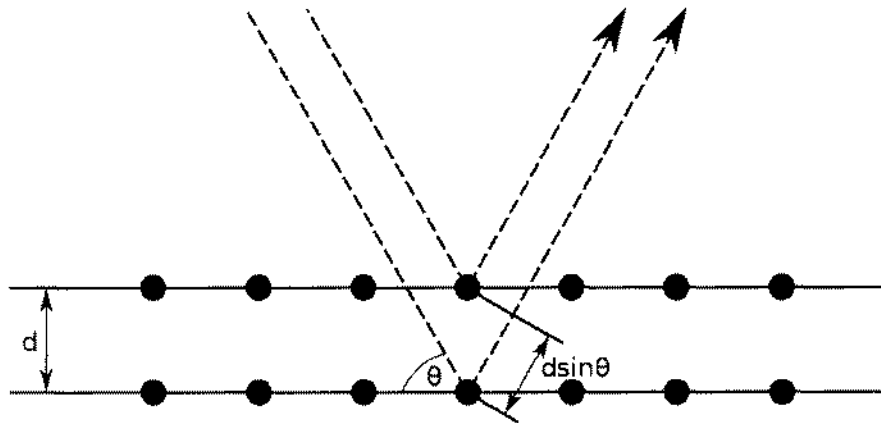


Figure 3.1 Bragg's diffraction law

By using Bragg's law, inter planner distance  $d$  can easily be calculated which are informative and a special source of 'fingerprint' for the minerals which exist in the sample, by the comprising of the calculated value of  $d$  with international standard, the materials can easily be identify by 'fingerprint'[54] of the sample. The 3-D nano amorphous compound structure is the regular and repeating lattice planes of the crystals. When a focused beam of X-ray fall on these atoms some of the X-rays diffracted with certain angle and the remaining X-ray are transmitted, refracted, reflected, absorbed by the target materials. The diffracted X-rays by the material act like just the sun light diffracted by water droplet in the atmosphere to form rainbow. The X-rays will diffract in different angle from each element present in the sample by the help of which each element surface can be studied. X-rays can be produced in a vacuum seal tub. A high energetic beam of electrons is allowed to fall on the target usually copper, to produce characteristic X-ray and then these X-rays were bombarded on the sample (films) for diffraction.

### 3.1.2 Spectroscopy.

A device with the help of which one can find transmission, absorption and reflection of light is called spectrometer. The instrument consists of a light source of known wavelength (visible or



UV) and a photometer to find out spectrum of the transmitted light from the sample. In spectrometer continues spectrum of band is passed but in a monochromator only one wavelength of spectrum is transmitted through the given sample and measure the intensity of transmitted light by the help of photometer [55].

If light falls on sample and some part “A “of the light is absorbed by the sample, some of the portion of light which is reflected by the sample is “R” and if “T” is the transmitted light then the total incident light intensity will be equal to the sum of all portion of light.

$$I_0 = A + R + T \quad 3.2$$

The relation between transmitted intensity “T” and incident intensity “I<sub>0</sub>” is called transmission “T” i.e.

$$T = I / I_0 \quad 3.3$$

While the relation between absorption and transmission is given by:

$$A = \log_{10} (I_0 / I) \quad 3.4$$

or

$$A = \log_{10} (I_0 / I) \quad 3.5$$

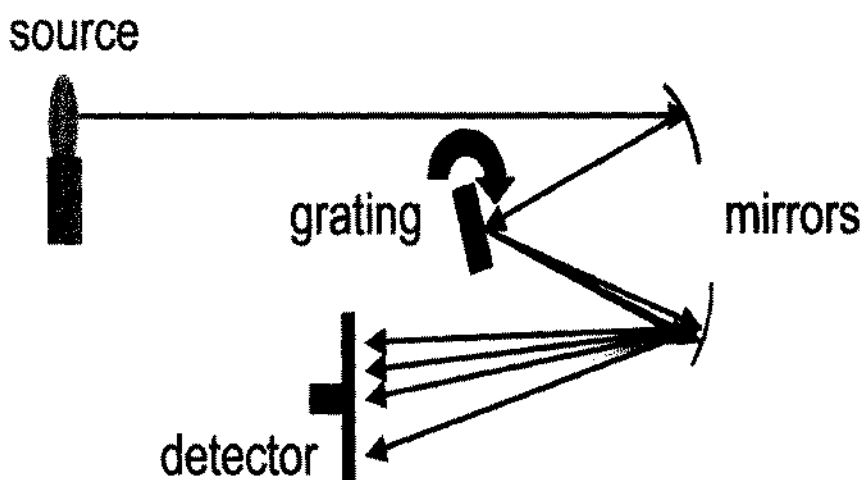


Figure 3.2 Schematic diagram of spectrometer

### 3.1.3 Fourier transformation infrared spectroscopy (FTIR).

It is [63] analytic technique which is used for an infrared spectrum of Reman effect, emission, absorption, photo conductivity of gas, liquid or solid. This type of spectrometer collects a

spectral data simultaneously in a wide clear spectral range. The principal of FTIR is based on Michelson interferometer. The diagram given below shows that maximum light is passes through interferometer because of zero path difference.

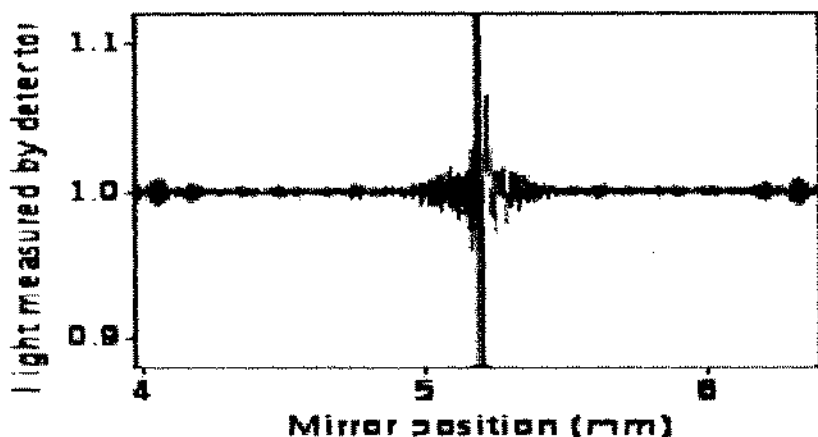


Figure 3.3 Interferometer of zero path difference.

FTIR originate from mathematical process which converts the raw data into spectrum form. The organic material is analyzed by using FTIR techniques. To identify small particles in a range of 10  $\mu\text{m}$ . FTIR microscopy is used. In such type of spectroscopy one can study interaction of infrared radiation with matter. The atoms of molecule and crystal continuously oscillate with natural frequency in a range of  $10^{13}$  to  $10^{14}$  Hz which is almost the frequency of infrared electromagnetic spectrum. Due to these oscillations there occur a change in dipole movement due to which absorption occur in infrared radiation. If the graph is plotted between radiation absorbed and incident radiation the graph will show the exact chemical bond. And hence may be used for identification of exact structure of the organic material. FTIR is most powerful available single technique for identifying qualitatively organic materials and for measuring molecular structure [57]. The schematic diagram of Michelson interferometer is shown below.

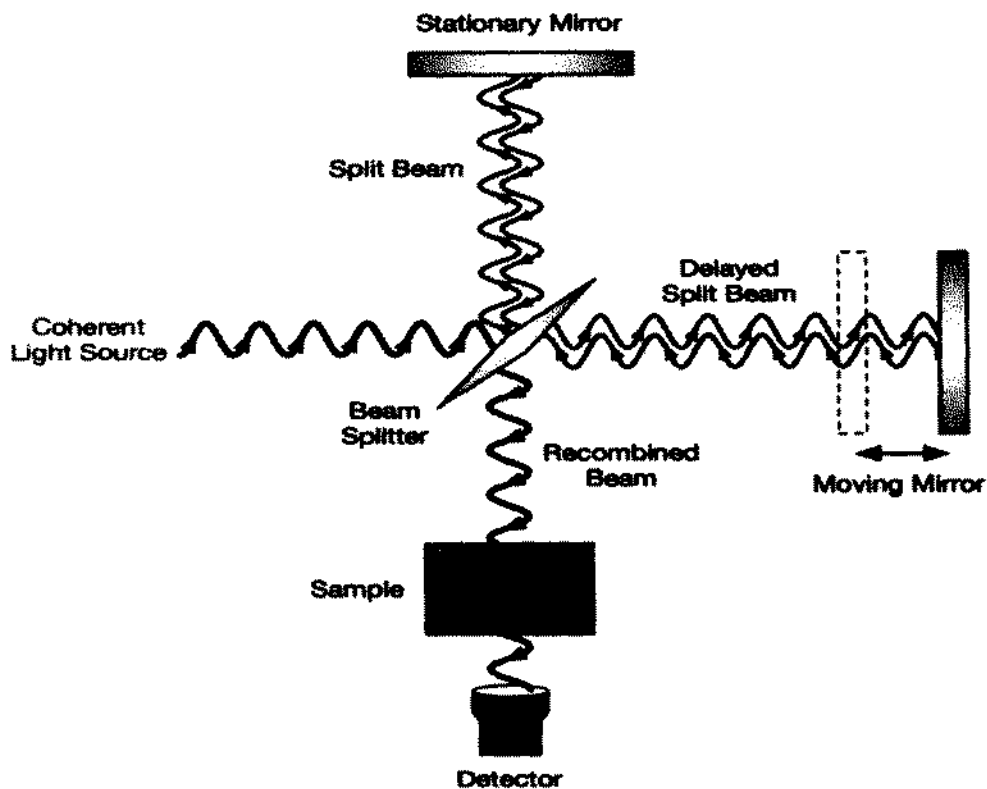


Figure 3.4 Schematic diagram of Michelson interferometer

### 3.1.4 Rutherford back scattering (RBS).

Rutherford back scattering is an analytical technique which is used to find out the bulk composition and structural surface of the materials by the bombardment of high energetic particles like hydrogen or helium/alpha particles. This was discovered by Hans Geiger and Ernest Marsden under the supervision of Rutherford while performing research on the bombardment of alpha particles on thin gold foil. During the experiments they observed that most of the alpha particles pass straight through the gold foil but few of them were deflected (in ratio of 1/10000) even in opposite direction i.e. at an angle of 180 degrees. According to Rutherford it was incredible that a 15 inch bullet is fired on tissue paper and bounces back by an angle of 180 degrees [58].

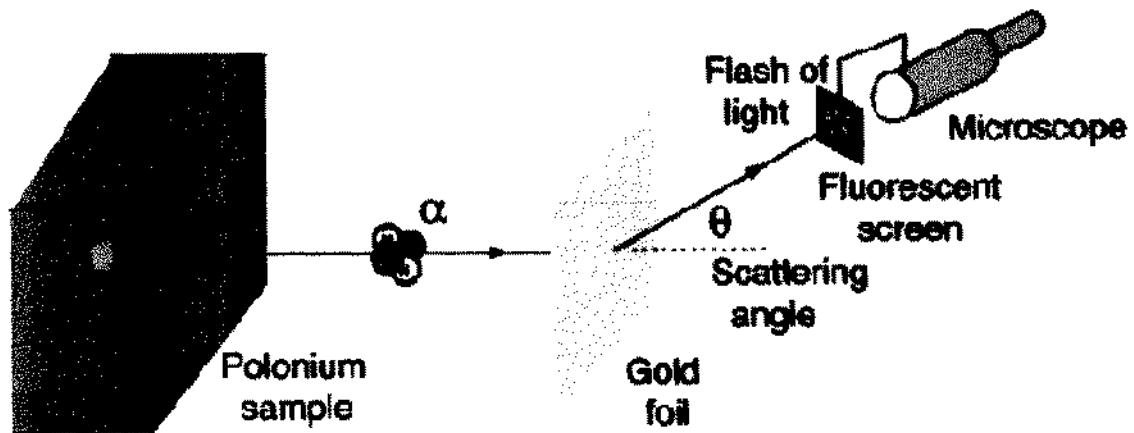


Figure 3.5 Schematic diagram of Rutherford back scattering

One can also use the following techniques to analyze the surface of thin films.

- ❖ Auger electrons spectroscopy (AES). In this technique the incident particles/projectiles are electrons and the deflected particles are once again electrons. i.e.

Electrons in → Electrons out

- ❖ Electrons microprobe analysis (EMA). In this technique the incident particles are electrons and X-rays are emitted. i.e.

Electrons in → X-ray out

- ❖ X-ray fluorescence spectroscopy (XRF). In this technique the projectile is X-rays and the outgoing is also X-rays. i.e.

X-rays in → X-rays out

- ❖ X-ray photoelectrons spectroscopy (XPS). In this type of technique X-ray is used as a projectile and electrons are out i.e.

X-ray in → Electrons out

- ❖ Secondary ion mass spectroscopy (SIMS). In this type of techniques the in and out particles are ion .i.e.

Ions in → ions out

Some of the techniques along with the above are shown in diagram in a complete order.

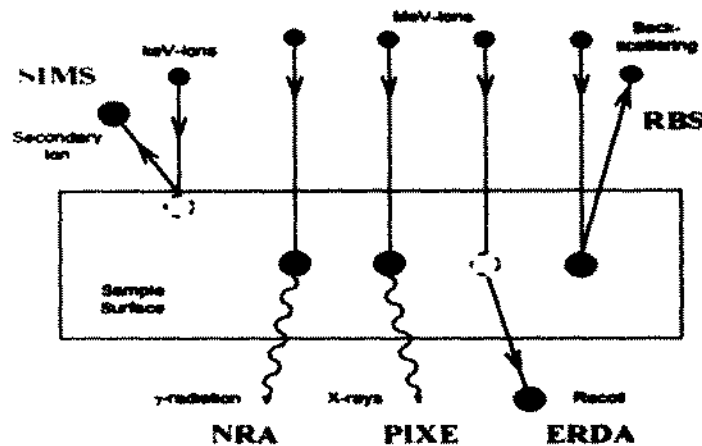


Figure 3.6 Schematic diagram of Analyzing techniques

Among the all of technique RBS is the most useful due to following reason.

- ❖ The best techniques for the surface analysis.
- ❖ A completely accurate and non damaging surface technique.
- ❖ With the help of this technique one can measure the exact thickness of thin films, depth and masses of materials present in a sample.
- ❖ Thin film crystalline quality.
- ❖ Impurities of lattice location in single crystal.
- ❖ Analyzed a film of thickness up to 2μm by using He ions and 20μm by using protons.
- ❖ Very sensitive for heave nuclei and less sensitive for lighter one.

The only disadvantage of RBS technique is the requirement of an expensive accelerator to accelerate the ions.

## Kinematic factor

During scattering the energy is lost in the form of momentum energy to the target atom. The ratio of the energy loss by the particles after scattering to the energy of the particles before scattering is called kinematic factor  $k$ . i.e.

$$k = E/E_0 \quad 3.6$$

Here “ $E_0$ ” is the energy of the particles before scattering and “ $E$ ” is the energy after scattering. By putting the values of ‘ $E$ ’ and ‘ $E_0$ ’ and solving for ‘ $k$ ’ equal to i.e.

$$k = \left( \frac{m_1 \cos \theta_1 \pm \sqrt{m_2^2 - m_1^2 (\sin \theta_1)^2}}{m_1 + m_2} \right)^2 \quad 3.7$$

Here particle 1 is the projectile, particle 2 is the target nucleus and  $\theta$  is the of angle scattering. If the projectile is backscattered from light nuclei present in the sample then there will be a much difference between those which scattered from heavy nuclei, due to the fact that a allot of energy is transferred from projectile to the light elements. Now if the masses of the elements of the target are increased than an extremely little amount of energy of the particles will be transferred. As a result loss in energy of the backscattered particles will asymptotically approaches to zero. This means that RBS is more useful to differentiate between two light elements as compare to difference between two heavy elements. The mass resolution of the light elements is very good, while the mass resolution of heavy elements is poor. The reason for this difference between light and heavy nuclei mass resolution is the amount of energy absorption. An important issue occurs during the backscattering of “ $\text{He}^{++}$ ” from proton or “ $\text{He}^{++}$ ” atoms in the sample. As the atoms are light or lighter than the bombarding particles or ions, instead of backscattering the particles will scattered in forward direction. So these particles will not be detected by the Detector in RBS. To detect such type of particles the detector will be adjusted in the forward direction and hence be detected.

## Thickness measurement of the layer

As in the backscattering process only small numbers of incident particles collide closely with atomic nuclei and bounce back from the sample. A large number of probing particles penetrate inside the sample to some extent of depth by losing some of their energy. So the particles backscattered from the surface have relatively high energy as compare to the particles backscattered from depth. This energy loss by the backscattered particles depends upon the compositions and densities elements in the sample. Which enables RBS to measure thickness of the film and the process is depth profiling.

### 3.1.5 Hall measurement effect.

This effect was discovered by Edven Herbert Hall [59], while working on a current carrying in a perpendicular magnetic field at university Bialtimor , Maryland[60]. According to this effect “The production of Hall voltage ( $V_H$ ) when a perpendicular magnetic field is applied to current carrying conductor”.

Mathematically:

$$V_H = - \frac{IB}{nte} \quad 3.8$$

Where “ $V_H$ ” is the Hall voltage “ $I$ ” is the current in conductor “ $B$ ” is perpendicular magnetic field “ $t$ ” is thickness “ $n$ ” is the charge carrier density and “ $e$ ” is the charge particles.

Hall Coefficient: It is a ratio of induced electric field “ $E_y$ ” to current density “ $J_x$ ” and a magnetic field “ $B$ ”. i.e

$$R_H = \frac{E_y}{j_x B} \quad 3.9$$

Where “ $R_H$ ” express Hall coefficient and unit is  $m^3/C$ , or  $\Omega \cdot cm/G$ .

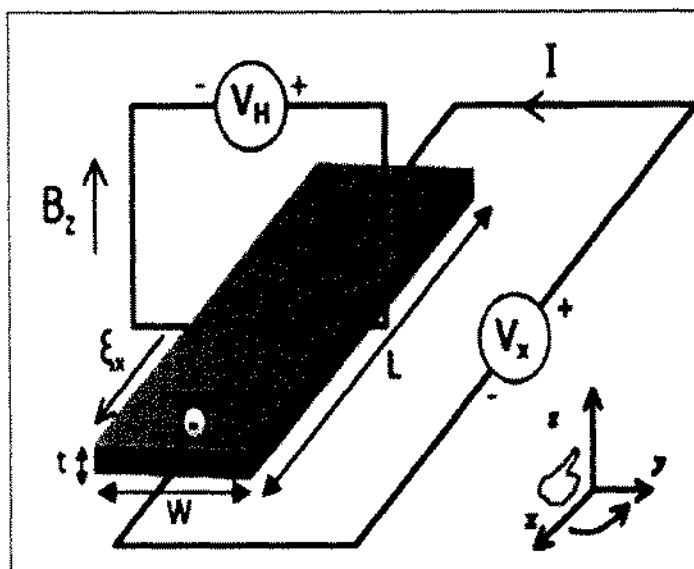


Figure 3.7 Schematic diagram of Hall Effect

It may be noted that if the magnetic field applied to the current carrying wire is not in a direction of current carrying wire the charge carrying wire will exert a force which is called Lorentz force [61] is given below.

3.10

Here ' $\vec{F}$ ' is the Lorentz force, ' $q$ ' is the charge particle, ' $\vec{E}$ ' is the electric field, ' $\vec{v}$ ' is the velocity and ' $\vec{B}$ ' is the magnetic field.

### 3.1.6 UV Visible Spectroscopy.

It is that type of technique which is used to know the optical properties of the sample (nano structural materials) or thin film. This technique work on absorption and reflection of light by sample which direct effect the color of the chemical (color is the physical property).The spectrometer consist of light emitting source in latest light emitting diode (LED) [62], reflecting mirror which reflect light and passes through a filter ,reach to a monochromater , now the light beam passes through beam splitter where the light is split in to two parts. The first one is collected directly after passing through reference and other portion of light passes through the sample and reach to detector. The intensities of both light measure by a detector. From this the



absorbance “A” is calculated by using “Beer Lambert” law. Which state that “Absorbance is directly proportional to the path length “L” of the sample and concentration of the absorbing species [63] i.e.

$$A \propto L \quad 3.11$$

$$A \propto C \quad 3.12$$

Combining the two equations i.e.

$$A \propto CL \quad 3.13$$

Or

$$A = \epsilon CL \quad 3.14$$

Also the absorption “A” is equal to.

$$A = \log_{10} (I_0/I) \quad 3.15$$

In the combine form i.e. 3.15 and 3.16 will be.

$$A = \log_{10} (I_0/I) = \epsilon CL \quad 3.16$$

Where “ $I_0$ ” is the intensity of the incident light “ $I$ ” is the intensity transmitted light, “ $L$ ” is the through sample, “ $c$ ” is the concentration of absorbing and “ $\epsilon$ ” is constant known extinction constant.

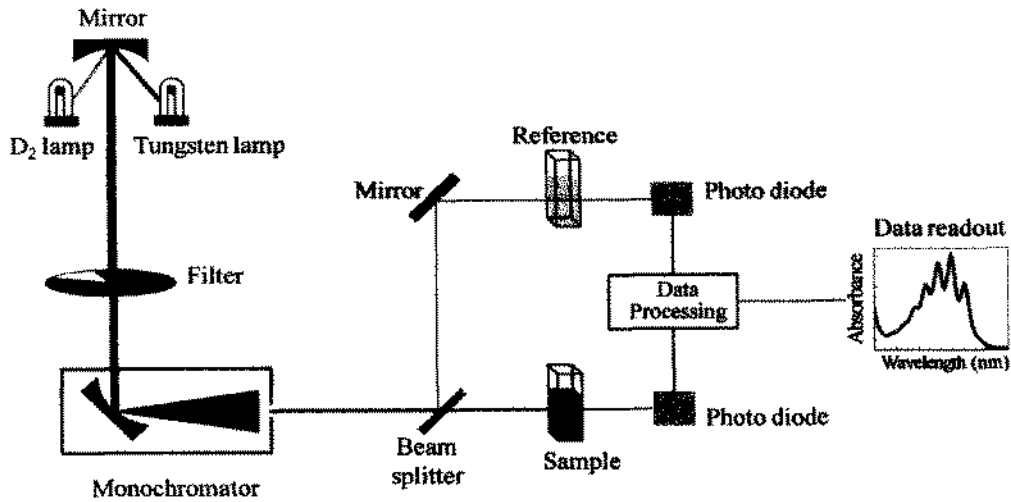


Figure 3.8 The schematic diagram of UV visible spectrometer

### 3.1.7 Defuse reflectance spectroscopy (DRS).

This is a technique which is used to find out the energy band gap and refractive index of the thin film. This type of technique is based on Defuse reflection i.e. the scattering of light in various directions from the surface of the film or the material under studying. Actually defuse reflection does not involve surface only but also the reflection of light takes place from inner of the surface also [67, 68].

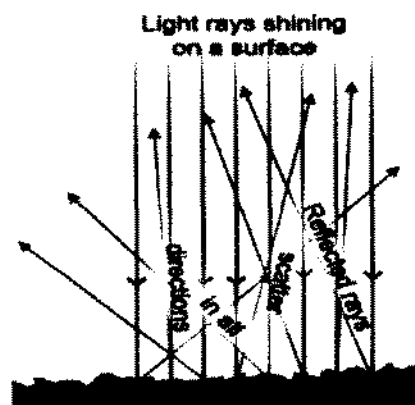


Figure 3.9 Schematic diagram of diffuse reflection

From any surface two type of reflection takes place i.e. Defuse reflection and Regular or Specular reflection (A reflection from smooth surface).Defuse reflectance spectroscopy is closely related to UV visible, but slightly different from each other i.e. in UV visible light is transmitted through liquids while in case of DRS light is reflected from the sample.

In DRS the light is reflected from the rough surface of sample and are collected through a collector and then analyzed. If the technique is applied to infrared (IR) region in the Fourier Transformation, then the spectroscopy is called DRIFTS or Kubelka-Mnnk due to their theory on radiation from the media scattering [69].Light falling on the materials (Film) surface is splits in to different part some of it is scattering in the form of specular reflection, some is in the form of defuse reflection and some of the light penetrate inside the material (sample).The portion which penetrate inside the sample may either be absorbed by the atoms of the sample or may be diffracted, which further giving rise to a diffuse diffraction. As specular reflection contort the spectra of DRS, thus the portion of specular reflection be neglected in diffuse measuring i.e. in DRIFTS the regular reflection is neglected.

## Chapter # 4

### Experimental Setup and Work

#### 4.1 Vacuum thermal evaporation.

Thin film of SnSbS were deposited on a clean clear from all type of contamination over glass substrate by using thermal evaporation method in a vacuum chamber as shown figure given below.

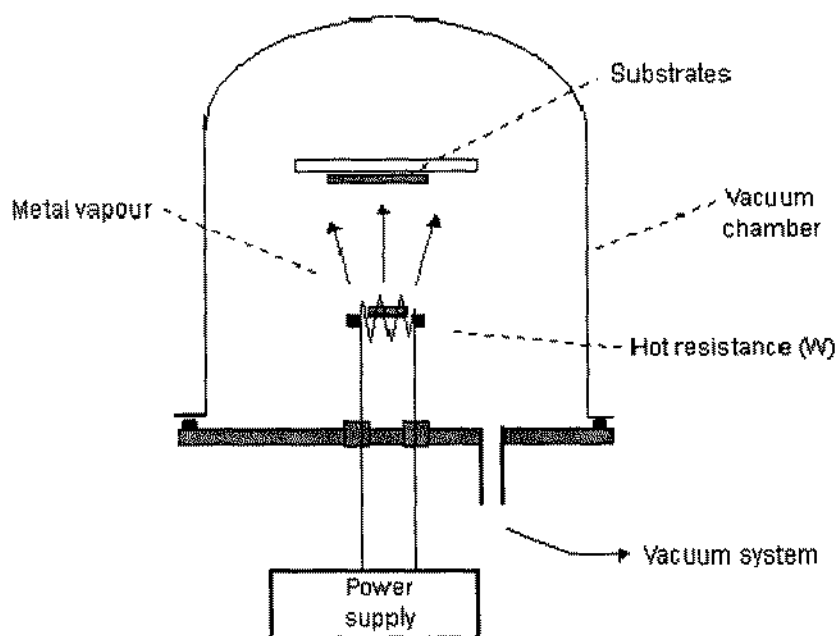


Figure 4.1 .Daigram of vacuum thermal evaporation.

**Theory.** In this type of technique the heating is continue until the evaporation of the base materials started and deposited over a clean and clear substrate from all type of contaminations . Usually for deposition technique a low pressure is used almost in range from  $10^{-6}$  to  $10^{-5}$  torr, to avoid from the reaction between atmospheric particles and the base material vapors'. At low pressure the vapors of the base material straight deposited over a cold substrate due the fact that the mean free path of base material vapors and that of vacuum chamber remain same. Different

methods can be used for thermal vacuum evaporation heat system. The apparatus available for this purpose in laboratories is either Joule heating affect i.e. Resistance heating.

Or

By the bombardment of high energetic electrons over base material to change the base material to vapors called Electron beam heating. The main component of thermal evaporator is given below.

- ❖ Chamber in cylindrical form.
- ❖ Rotatable substrate receptacle.
- ❖ Physical thickness observer.
- ❖ Optical thickness observer.
- ❖ High D.C. supply.
- ❖ Dual level vacuum pumps.
- ❖ Gas flow regulator.
- ❖ Heating system for substrate.
- ❖ Diffusion and rotary pumps.
- ❖ Cooling system.
- ❖ Resistive boards.

#### **4.2 Material used for sample preparation.**

Pure powder of SnS and  $Sb_2S_3$  (99.99% both) simultaneously evaporated in a vacuum chamber. A thin film of SnSbS were deposited on a clean clear glass substrate and then copper nitrate were solved in ultra high pure water and SnSbS films were dipped into the solution for at least 20 minutes dried and annealed for 20-30 minutes at  $160^{\circ}C$ . All the materials are easily available in local market.

#### **4.3 Substrate selection.**

The best substrate used for the deposition of thin film is quartz as compare to glass substrate. But in comparison to glass it is expensive and not easily available in the local market, therefore we used glass substrate for deposition of thin film.

A best substrate among all is one that whose surface is very smooth or extra smoothes, has high melting point, high power of resistivity, a suitable mechanical strength, zero porosity and is of very low cost.

#### **4.4 Substrate cleaning.**

To clean and free the substrate from all types of contamination the following steps can be followed.

1. Clean the substrate for 5-10 minutes ultrasonically in acetone.
2. Wash in ultra high pure water in 3-5 minutes.
3. Cleaning for at least 3 minutes in methanol.
4. Finally clean ultrasonically in propanol vapors at 100 °C and dry.

OR

One can also use the following steps to clean substrate from all types of contamination by using the following steps.

1. Chemical storage.
2. Mix organic solution.
3. Mix ionic solution.
4. Mix HF solution.
5. Setup bubbler reins.
6. Organic clean.
7. Oxides clean.
8. Ionic clean.
9. Transporting substrate.
10. Drying.

##### **1. Chemical storage.**

The chemical which are used for cleaning process are placed just below the work area. It may be remember that the solvent and acids are placed separately in a store chamber. Each time a fresh chemical solution is used at the same time to avoid for delay in cleaning.

##### **2. Mix organic solution.**

Using precautionary steps protecting eyes, wearing gloves, the organic solution is prepared i.e. taking 1000 ml of deionizde water in a quartz vat (vessel) in a 200 ml hydrogen per Oxide.

Along with addition of 200 ml ammonium hydrogen. Now put the vessel over a heater and adjust the temperature at 350 °C. The solution need to be at 80 °C for at least 15 minutes.

### 3. Mix ionic solution.

Next step to mix organic solution is mix organic solution. This can be prepared in different container for the sake of avoiding cross contamination. We follow the same methods that we used in mix organic solution but instead of ammonium hydrogen this time we used HCL and similarly follow the remaining steps and reach to the final that is to dry the substrate. I used the first one method for its simplicity and cheapness.

### **4.5: preparation of tin antimony sulfide doped with copper ion thin film.**

Tin doped Antimony Sulfide was deposited on the clean and clear glass substrate by using thermal evaporation technique in a vacuum chamber. Initially the substrate was fixed in a holder just above the source material in a vacuum chamber with the help of rotary pump. The pressure of the chamber was reduced to  $10^{-1}$  mbar and then with the help of diffusion pump the pressure of the vacuum chamber was reduced to  $10^{-5}$  mbar. Both source materials i.e. SnS and  $Sb_2S_3$  were highly in pure form i.e. 99.9 % pure. SnS was prepared from the powder of sulfur and Tin according to the scheme and reference [64, 65].

Sn and S were mixed in a ratio of 0.7873 gram to 0.2127 gram in a respectively crushable and annealed for 24 hours at 600 °C in a quartz ampoule containing organ gas and then to homogenize completely Tin Sulfide, the ampoule was left free to cool slowly. A highly (99.9 %) pure form of  $Sb_2S_3$  were obtained from sigma Aldrich (kurt J.Lesker).

Both the powered SnS and  $Sb_2S_3$  were evaporated simultaneously from  $Al_2O_3$  boat for a thin film deposition over a glass substrate in a vacuum chamber by keeping the pressure in a range of up to  $10^{-5}$  mbar. The thickness of the film deposited on a glass substrate obtained is in a range from 300nm to 700 nm. The film was then annealed in a presence of organ gas up to 150°C. Now the Tin antimony Sulfide thin film was cut into different pieces. Now these thin films were dipped into copper nitrate solution with ultra high pure water for at least 20 minutes. In which the copper ions were doped into the thin film and then the film were dried in and annealed for at least 20 minutes in electric furnace over temperature of 150 °C and then the electric furnace was allowed to cool slowly. Now finally the films were ready for characterization.

## Chapter # 5

### Results and discussions

#### 5.1 Rutherford backscattering Spectroscopy (RBS).

Rutherford back scattering spectroscopy (RBS) is one of the best surface analysis techniques among the available to measure the composition and thickness of thin films. The RBS of the films have been performed at National Centre for Physics (NCP) Islamabad with the kind support of Dr Ishaq in December 2014. The parameters which were used for Rutherford backscattering spectroscopy (RBS) are given below.

Accelerator : 5MV pelletron Tandem Accelerator NCP

Beam : He<sup>++</sup>

Energy : 2.084 MeV

Current : 28 nA

Charge : 15  $\mu$ C

Detector Type : Solid State Barrier

Detector Resolution: 20 KeV

Incident angle : 0 deg.

Beam diameter. 2mm.

Backscattering angle: 170 deg.



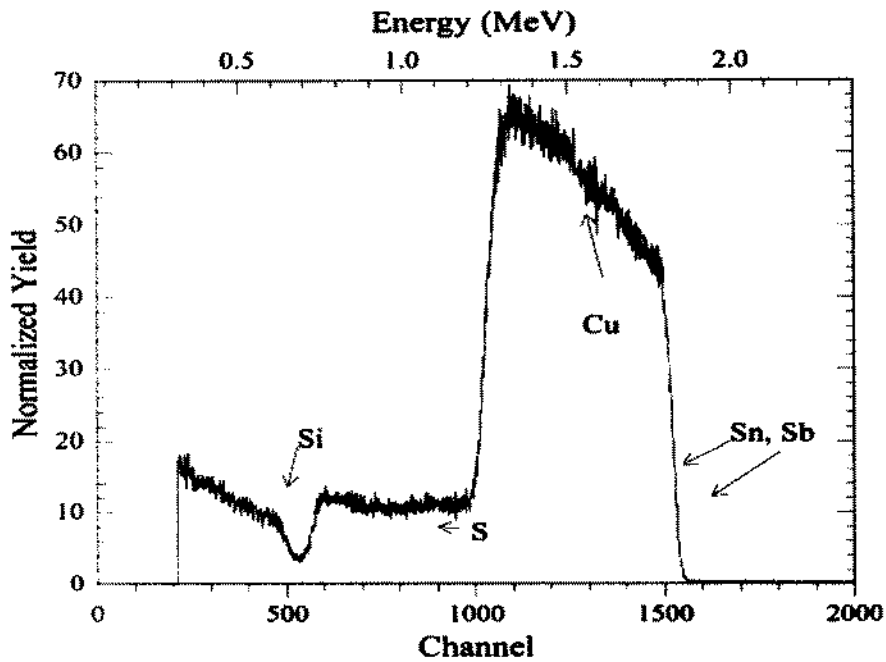


Figure 5.1 Graph of Channel/Energy and Normalized Yield of Sample 1

Figure 5.1 shows the experimental data of sample of thickness 240nm with copper concentration 2.94%. The energy of the  $\text{He}^{++}$  used was 2.084MeV, the incident and backscattering angles were 0 degree and 170 degree.

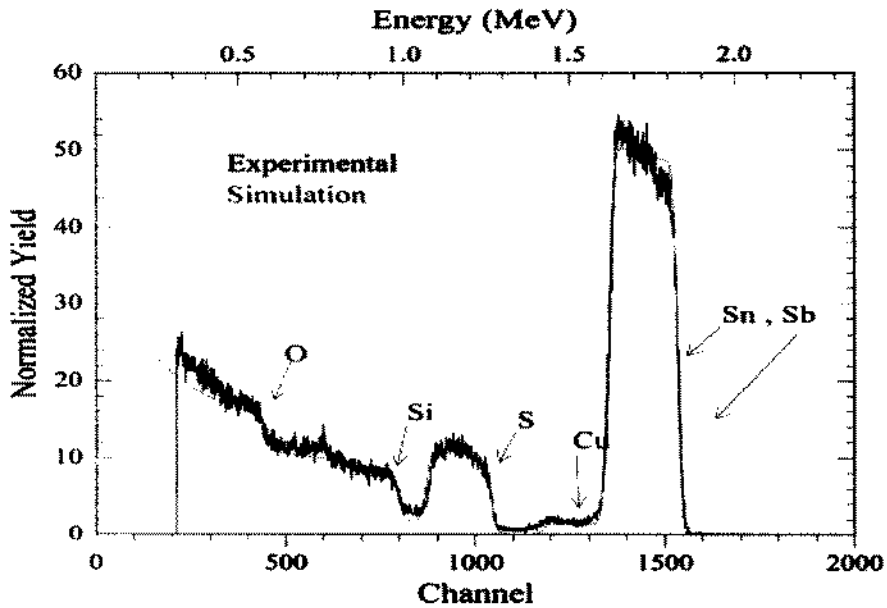


Figure 5.2 RBS Graph of simulated and experimental

Figure 5.2 shows the comparison of measured and simulated spectra of sample of thickness 240 nm with doping of 2.49% copper. The simulated spectra cover the measured spectra very well.

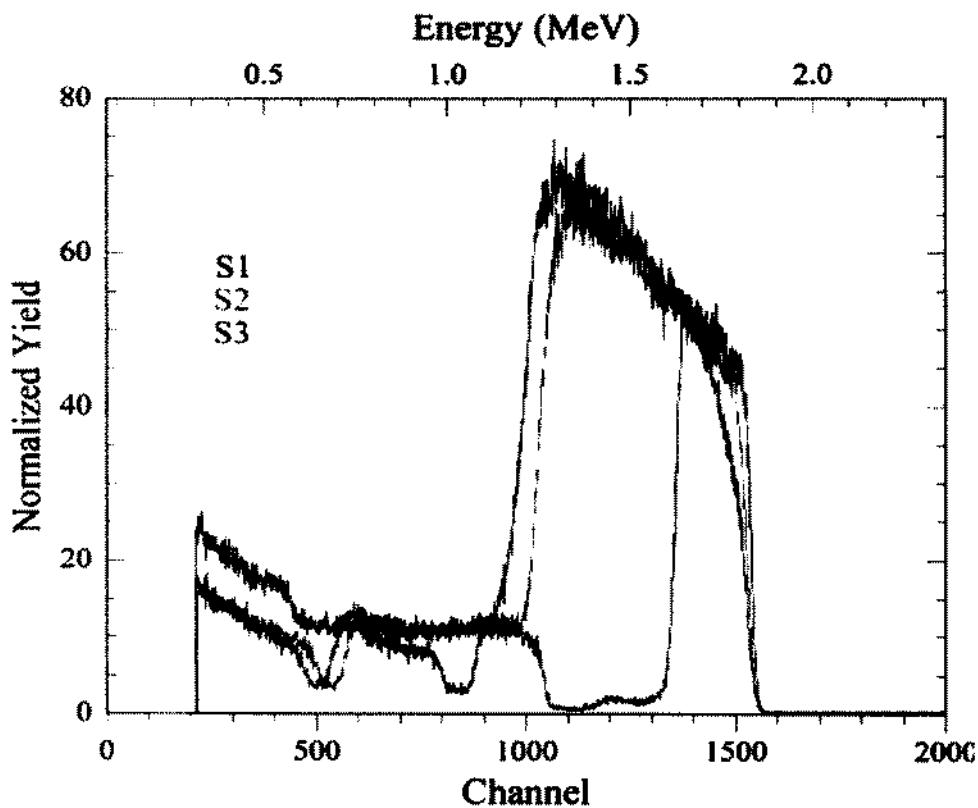


Figure 5.3 Comparison RBS spectra of all samples

Figure 5.3 shows the comparison of all the samples. Here ' $S_1$ ' is the graph of sample number one whose thickness is 240 nm and copper concentration is 2.49%, ' $S_2$ ' is the graph of sample number two whose thickness is 690 nm and copper concentration is 2.93% and ' $S_3$ ' is the graph of sample three whose thickness is 730 nm while copper concentration is 3.56 %.

**5.1.1 Thickness and composition of elements in the films.** The thickness and composition of elements in the sample along with the thickness and composition of the elements of the substrates were found with Rutherford back scattering spectroscopy and are given in the table 5.1.

Table 5.1 Thickness and elemental composition

S.No	Thickness (nm)	Composition in Percentage			
<b>Substrate</b>					
01	3000	Silicon (Si)	Oxygen (O)	Calcium (Ca)	Sodium (Na)
		33.43%	61.39%	3.34%	1.52%
<b>Thin film</b>					
02	240	Tin (Sn)	Antimony (Sb)	Sulfur (S)	Copper (Cu)
		14.09%	26.79%	56.63%	2.49%
03	690	13.29%	26.63%	57.16%	2.93%
04	730	13.84%	27.12%	55.48%	3.56%

## 5.2 The Hall Effect measurements.

Hall apparatus ECOPIA HMS-5000 in NUST was used to find out Hall Effect measurements. in the presence of constant magnetic field of 0.5Tasla at room temperature of thin films. The apparatus is fixed on a magnetic field of 0.5 Tesla at room temperature. The following parameters were calculated from the system. In which the most important one is the carrier mobility thin films as well for solar cell technology.

1. Mobility.
2. Charge carriers.
3. Conductivity.

4. Resistivity.
5. Bulk concentration.
6. Sheet concentration.
7. Magneto Resistivity.
8. The hall voltage.

### 1. Mobility.

The electrons or hole mobility is the ratio between drift velocity “ $V_d$ ” and electric field “ $E$ ”.

$$\mu_{e,h} = \frac{V_d}{E} \quad 5.1$$

Here “ $\mu_{e,h}$ ” is mobility and unit is  $(m^2V^{-1}S^{-1})$ .

### 2. Charge or carrier concentration.

The carrier concentration is the number of free electrons or holes in the conduction or valence band. In solar cell the carrier concentration play the most important rule.

### 3. Conductivity.

This is the characteristic of the conductor which allow current. The reciprocal of resistivity is called conductivity. It is denoted by “ $\sigma$ ” sigma and its SI unit is Siemens/meter (S/m). or  $(Ohm)^{-1}(meter)^{-1}$ . In term of electric field ‘it is a ratio between electric field and current density. i.e.

$$\sigma = \frac{E}{J} \quad 5.2$$

Where  $E, J$  represent electric field and current density.

**4. Resistivity.** This is the intrinsic property of the materials and shows the resistance toward the flow of current, and as define as the reciprocal of conductivity is called resistivity. This can also be define from Pouillet’s i.e.

$$\rho = R \frac{A}{L} \quad 5.3$$

Where  $\rho, R, A$  and  $L$  are resistivity, resistance, area and length f the materials respectively.

**5. Bulk concentration.** The bulk concentration of the material is the total concentration of the charge particles in the material in absence of electric current.

**6. Sheet concentration.** Bulk concentration of the material is the total concentration of the charge particles, while sheet concentration is just the concentration of charge particles at the surface of film.

7. **Magneto resistivity.** This is the property of the material which changes the electrical resistivity by the application of external magnetic field.

8. **Charge or carrier concentration.** The carrier concentration is the number of free electrons or holes in the conduction or valence band. In solar cell the carrier concentration play the most important rule.

The calculated values of Hall measurements are given in tables 5.2, 5.3 and 5.4 below.

Table 5.2 Hall measurements for sample 1

S/no	Current in Ampere.	Bulk concentration. [cm <sup>-3</sup> ]	Sheet concentration. [cm <sup>-2</sup> ]	Resistivity.(ρ) [Ωcm]	Conductivity. (σ) . [1/Ωcm]	Mobility.(μ) . $\frac{cm^2}{Vs}$ .
1.	1.0E-9	-7.017E+10	-1.684E+6	3.043E+12	3.287E-13	2.923E-5
2.	1.0E-6	4.196E+12	1.007E+8	1.583E+8	6.318E-9	9.400E-3
3.	1.0E-3	The values were not obtained due to high resistivity				
4	1.0E-2					

Table 5.3 Hall measurements for sample 2

S/n o	Current in Ampere.	Bulk concentration. [cm <sup>-3</sup> ]	Sheet concentration. [cm <sup>-2</sup> ]	Resistivity. (ρ) [Ωcm]	Conductivity. (σ) . [1/Ωcm]	Mobility. (μ) . $\frac{cm^2}{Vs}$ .
1	1.0E-9	5.973E+12	4.121E+8	7.736E+4	1.293E-5	1.351E+1
2	1.0E-6	-7.466E+14	-5.151E+10	6.677E+7	1.478E-8	1.236E-4
3	1.0E-3	3.787E+18	2.623E+14	6.315E+5	1.583E-6	2.6160E-6
4	1.0E-2	-7.268E+17	-5.015E+13	2.0602E+0	3.844E-1	3.301E+0

From table 5.3 one can easily check that by increasing current from 1nA to 1cA the value of resistivity /resistance decreases while the value of conductivity and mobility i.e. charge carriers increases. So from this it is clear that if a fraction (2.93%) of copper (Cu) is doped to Tin Antimony sulfide thin film efficiency increases.

Table 5.4 Hall measurements for sample 3.

S/no	Current in Ampere.	Bulk concentration. [cm <sup>-3</sup> ]	Sheet concentration. [cm <sup>-2</sup> ]	Resistivity. ( $\rho$ ) [ $\Omega\text{cm}$ ]	Conductivity. ( $\sigma$ ) [ $\frac{1}{\Omega\text{cm}}$ ]	Mobility. ( $\mu$ ) [ $\frac{\text{cm}^2}{\text{Vs}}$ ].
1	1.0E-9	2.330E+12	1.701E+8	3.653E+4	2.737E-5	7.334E+1
2	1.0E-6	-6.776E+13	-4.946E+9	5.683E+2	1.760E-3	1.621E+2
3	1.0E-3	-1.292E+17	-9.428E+12	4.589E-1	2.179E+0	1.053E+2
4	1.0E-2	-5.519E+17	-4.029E+13	4.136E-2	2.418E+1	2.735E+2

From table 5.4 it is clear that as the values of currents increases from 1nA to 1cA the values of resistivity decrease while conductivity and mobility increases .The doping percentage of copper this time was 3.56%. It may be noted that the reading of the Hall measurements were taken at 300k.

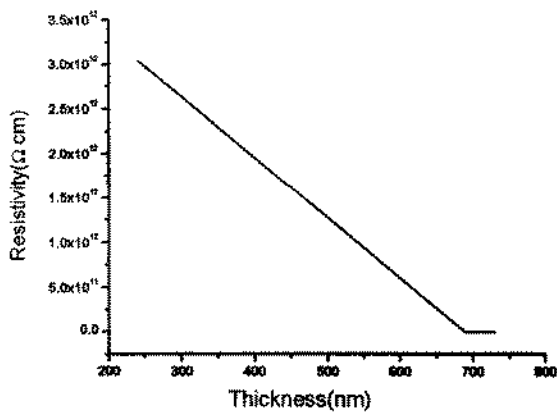


Figure 5.4 Graph of 1nA (Resistivity and Thickness)

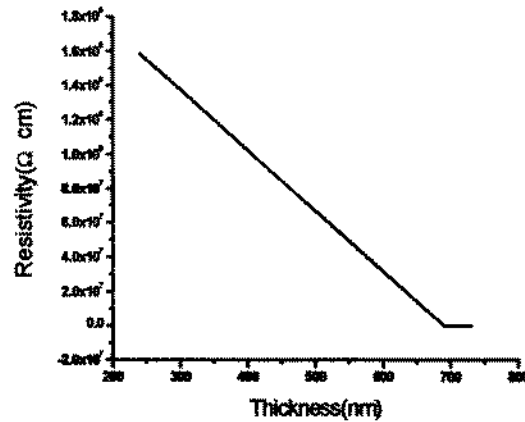


Figure 5.5 Graph of 1μA (Resistivity and Thickness)

The above figures i.e. 5.4 and 5.5 shows that with increase of thickness and copper concentration the resistivity of the films decreases.

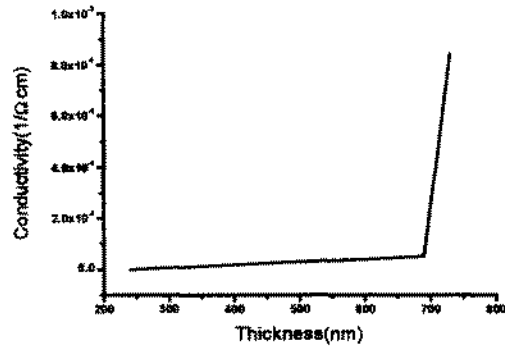
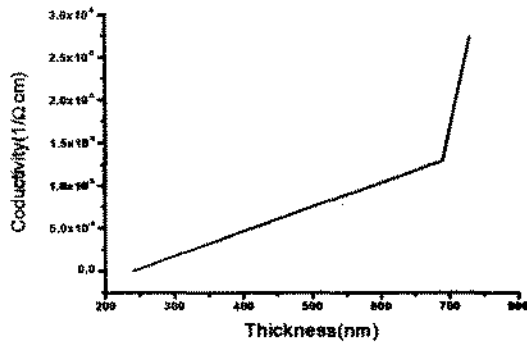


Figure 5.6 Graph of 1nA (Conductivity and Thickness)      Figure 5.7 Graph of 1 $\mu$ A  
(Conductivity and Thickness)

Figure 5.6 and 5.7 is the comparison between thickness and conductivity of the films, which shows that with the increasing thickness and copper concentration the conductivity of the films increases.

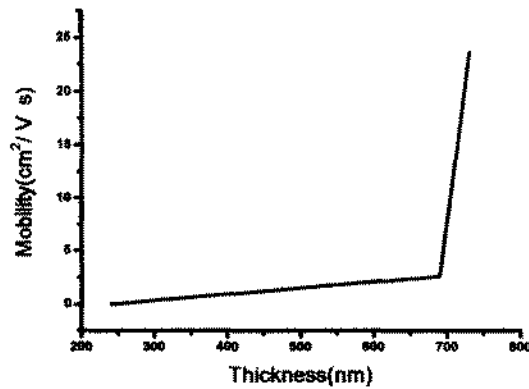
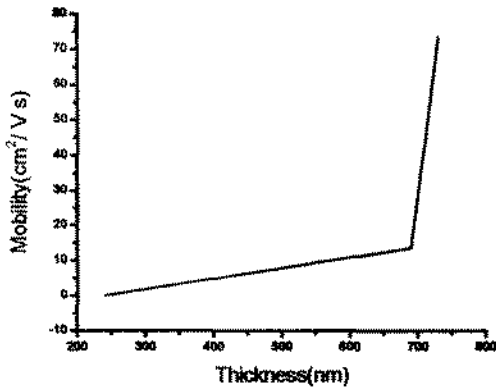


Figure 5.8 Graph of 1nA (Mobility and Thickness)      Figure 5.9 Graph of 1 $\mu$ A (Mobility and  
Thickness)

The above two figures shows that with the increasing thickness and copper concentration the mobility (charge carriers) increases.

### 5.3 Structural Properties.

To study the structural properties of SnSbS thin films doped with copper the XRD pattern of the film were obtained, which are shown in the Figure's 5.10, 5.11, 5.12, 5.13 and 5.14. The XRD of as deposited film shows amorphous structure before annealing were. XRD is one of the most important techniques used in material science and chemistry. With the help of XRD one can easily study the structure i.e. crystallite size and shape of the non structural materials unit cell. Diffraction method is helpful for both quantative and qualitative analyses.

#### 5.3.1 Indexing.

The first step in the XRD technique is called indexing i.e. the process by which the dimensions of unit cell determined from the peak position is called Indexing. For Indexing of any XRD pattering it is important to mark each peak position to Miller indices i.e. (h k l).It is not so easy just like picking the peak position of unit cell dimension and wavelength [70].The XRD pattern are in good agreement with a standard (JCPDS) database card number 35-1496 [71].The crystalline structure were found to be an orthorhombic.

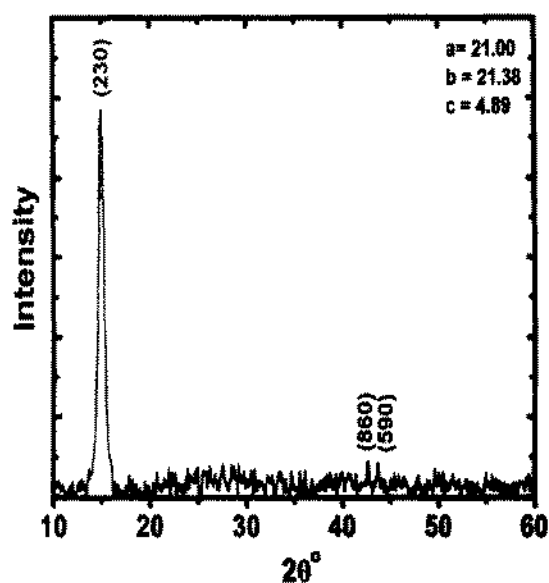


Figure 5.10 XRD pattern of sample i

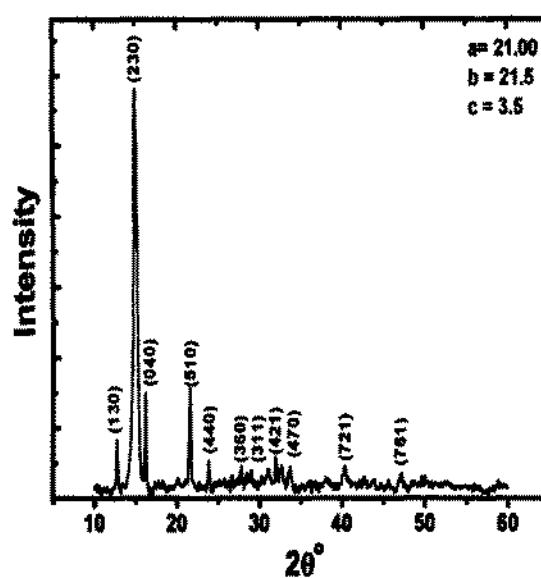


Figure 5.11 XRD pattern of sample ii



$$D = \frac{K\lambda}{\beta \cos \theta}$$

The average particle size can be calculated by using Scherer's formula [72-75] i.e.

### 5.3.2 Calculation of Grain size.

Figure 5.14 XRD patterns of all samples (i, ii, iii and iv)

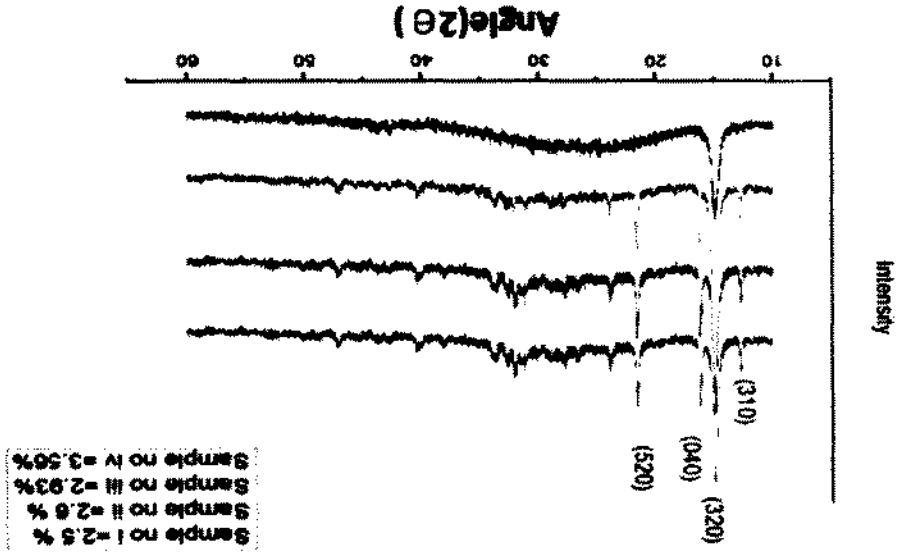


Figure 5.13 XRD pattern of sample iv

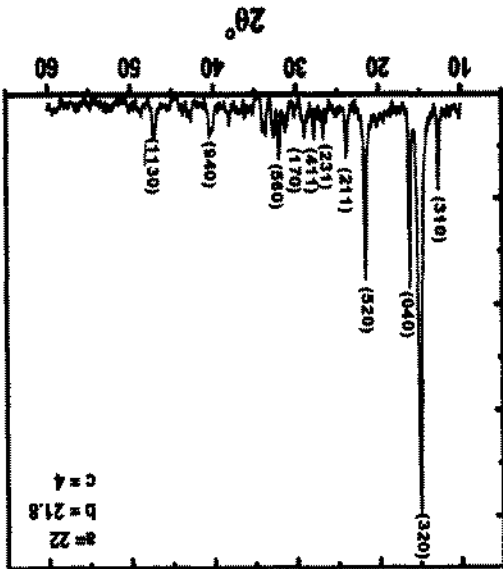
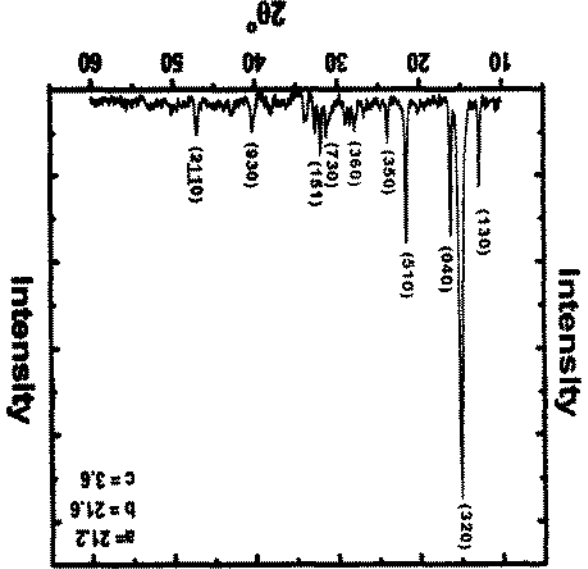


Figure 5.12 XRD pattern of sample iii



Where 'D' is the diameter of the particle, 'k' is the constant and its value is taken in this case 0.9, 'λ' is the wavelength of the x-rays used of value in this equal to 1.5490Å, 'β' is the full wave width at half maximum(FWHM) and 'θ' is the Bragg's angle at peak position.

### 5.3.3 Inter planning distance 'd'.

The inter planner distance can be calculated by using Bragg's law [76, 77] i.e.

$$2d \sin \theta = n\lambda \quad 5.5$$

Here 'd' is the inter planning distance, 'θ' is the angle of diffraction, 'n' is the number of order whose values may be 1, 2, 3, 4..... and 'λ' is the wavelength of x-rays.

### 5.3.4 Micro strain.

Micro strain is the mechanical properties of thin film which can be calculated by using a relation given below.

$$\epsilon = \frac{\beta \cos \theta}{4} \quad 5.6$$

Here 'ε' is for micro strain, 'β' is full wave at half maximum (FWHM) and 'θ' is the peak position angle.

### 5.3.5 Dislocation density.

Dislocation density of thin film is the imperfection and be calculated by using Williamson and Smallman's equation.

$$\sigma = \frac{n}{D^2} \quad 5.7$$

Here 'σ' denote Dislocation density, 'n' here equal to one and 'D' is the grain size.

Table 5.5 Calculated values of Grain size, Micro strain, Dislocation and Inter planer distance

S/no	Copper (%)	Two theta (2θ)°	FWHM 'β'	Grain size 'D' (nm)	Micro Stain 'ε'	Dislocation 'σ'	Interplaner Spacing 'd'(Å)
1	1.52%	14.936	0.6720	11.9	0.16657	7.0616E-3	5.92758
2	-	14.913	0.3542	33.33	0.08701	9.002E-4	5.94061
3	2.49%	14.976	0.3542	38.2	0.17558	6.853E-4	5.9122
4	2.93%	15.0169	0.3149	38.8	0.07804	6.643E-4	5.89977

In the Table the angle  $2\theta$ , Grain size, Micro strain, Dislocation and Interplaner distance are given at the peak position of all graphs. The average grains size in each samples were i.e. 11.9nm, 33.3nm, 38.2nm 38.8nm.for the samples 1, 2,3and 4 respectively

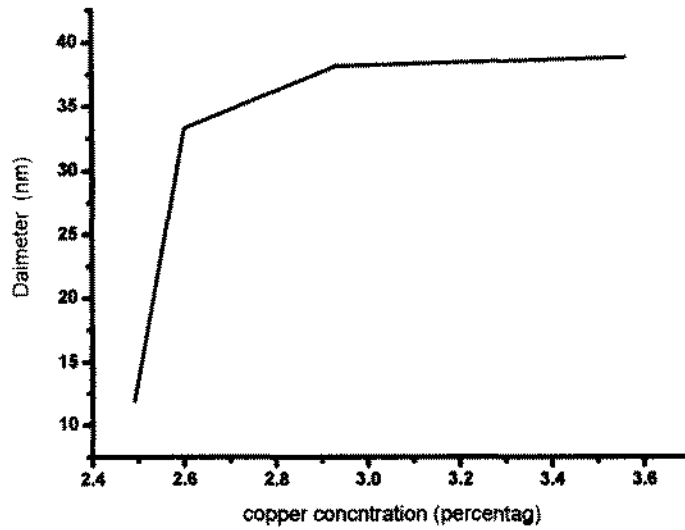


Figure 5.15 Graph of Copper (%) and Diameters (nm)

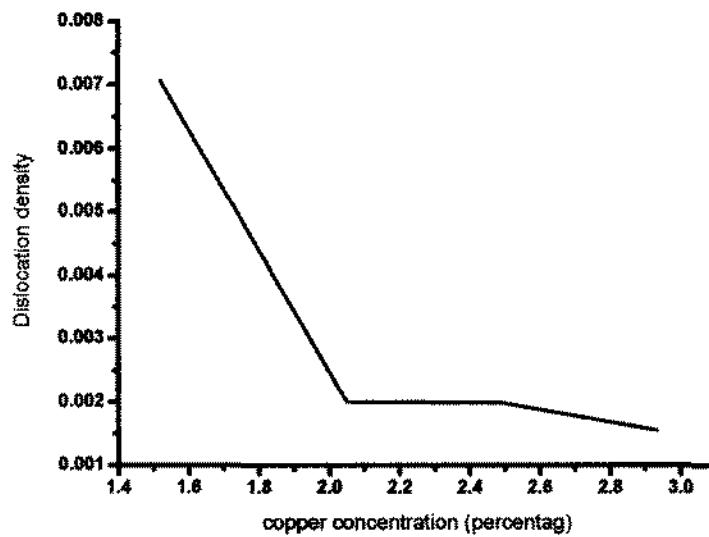


Figure 5.16 Graph of copper (%) and Dislocation Densities

## 5.4 Optical characterization.

### Transmission

The optical transmission spectra of the films were measured in COMSAT within a range of 300 to 1200nm by using Hitachi U-4001 Spectrometer, the transmission spectra of all the samples are shown in figure.

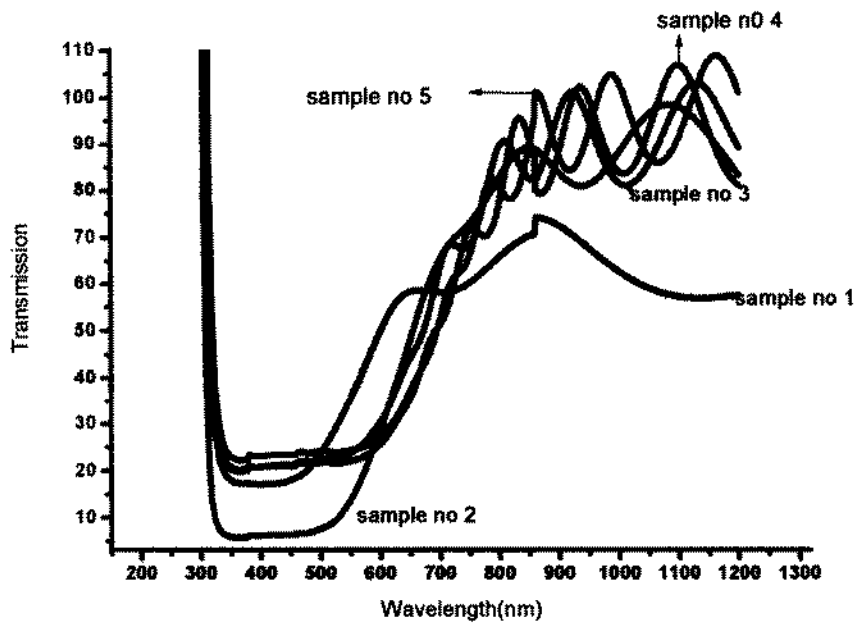


Figure 5.17 Graph of as deposited Transmission of all samples

The maxima and minima in the interference pattern help us to calculate the refractive index and thickness of the films can be calculated by using Swanpoel method [78-80]. The following formula was used to calculate the refractive index of the films.

$$n = \sqrt{N + \sqrt{N^2 - S^2}} \quad 5.8$$

Here 'n' is the refractive index of the film, 'N' is the number and 'S' is the refractive index of the substrate. For calculating 'N' the following relation was used.

$$N = 2S \left( \frac{T_{max} - T_{min}}{T_{max} T_{min}} \right) + \frac{S^2 + 1}{2} \quad 5.9$$

Here ' $T_{max}$ ' is the extreme top peak of transmission, ' $T_{min}$ ' is the extreme lower peak of transmission and ' $S$ ' is the refractive index of the substrate used.

The films thickness was calculated by using a formula given below.

$$d = \frac{1}{4n} \left[ \frac{\lambda_{Max}\lambda_{min}}{\lambda_{max}-\lambda_{min}} \right] \text{----- 5.10}$$

Here ' $d$ ' is the thickness of the film, ' $n$ ' is the refractive index of the film, ' $\lambda_{max}$ ' is the maximum wavelength and ' $\lambda_{min}$ ' is the minimum wavelength in the transmission spectra.

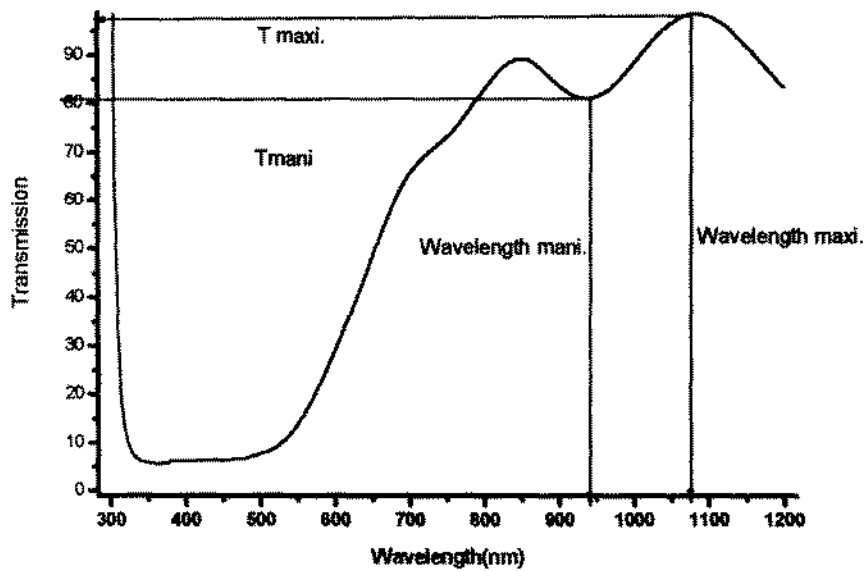


Figure 5.18 Graph shows maxima and minima of Transmission and Wavelength

Here in figure 5.18  $T_{maxi}$  is the transmission at maximum wavelength and  $T_{mani}$  is the transmission at minimum wavelength.

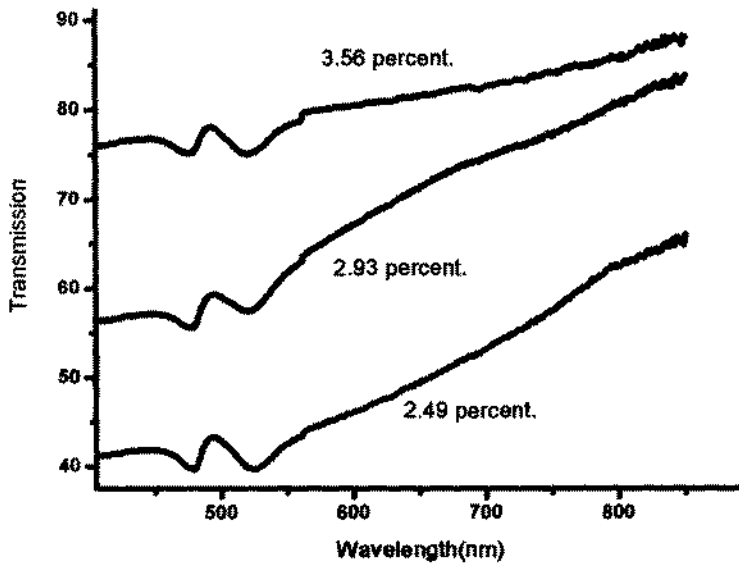


Figure 5.19 Transmissions Spectra after doping

The calculated value of refractive index of one of the film is 2.24 which is an agreement with the value of tin antimony sulfide and thickness of the same film by using equation 5.10 equal to 790 nm. Which may be confirmed from Table 5.1 on page 35 already calculated by RBS method and is equal to 730 nm. The calculated values of refractive index are given in the table.

Table 5.6 Copper concentration and calculated values of Refractive index

s/no	Copper (%)	$T_{maxi}$	$T_{mani}$	Refractive index
1	0	0.9705	0.8859	2.24
2	2.49	0.4324	0.3974	2.082
3	2.93	0.5926	0.5576	1.90
4	3.56	0.7807	0.7509	1.77

From Table 5.6 it is clear that with the increase of copper concentration the refractive index of the film decreases.

### Reflectance spectra.

Optical reflection spectra of tin antimony sulfide doped by copper is shown in 5.20, 5.21 and 5.22 Figures .The graph of each film in which percentage ratio of copper doping is different i.e. from 2.49% to3.56%. Reflection spectra were measured by DRS (T-90 UV Spectrometer) in a range of 199nm to 850nm in National center in of physics (NCP) Islamabad.

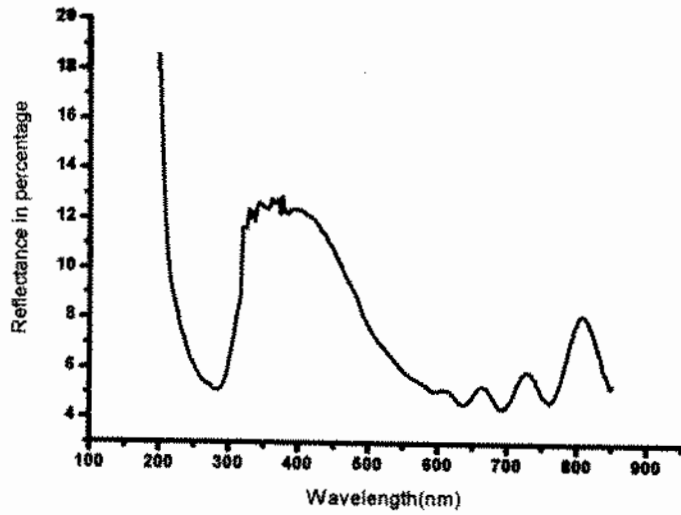


Figure 5.20 Graph of sample thickness 240nm and doping of copper 2.49%.

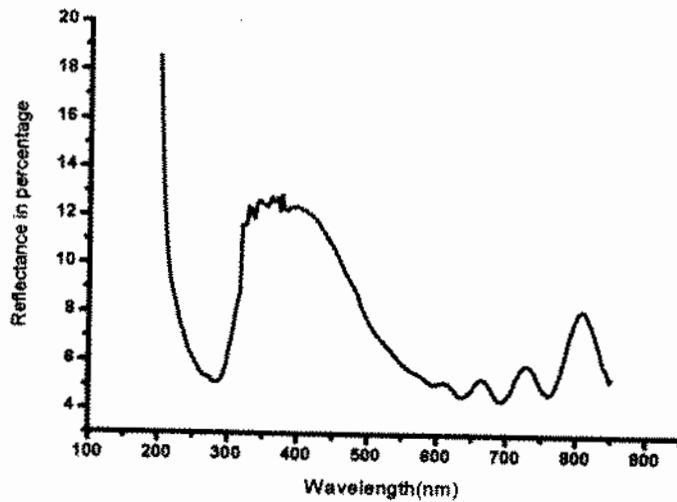


Figure 5.21 Graph of sample thickness 690nm and doping of copper 2.93%.

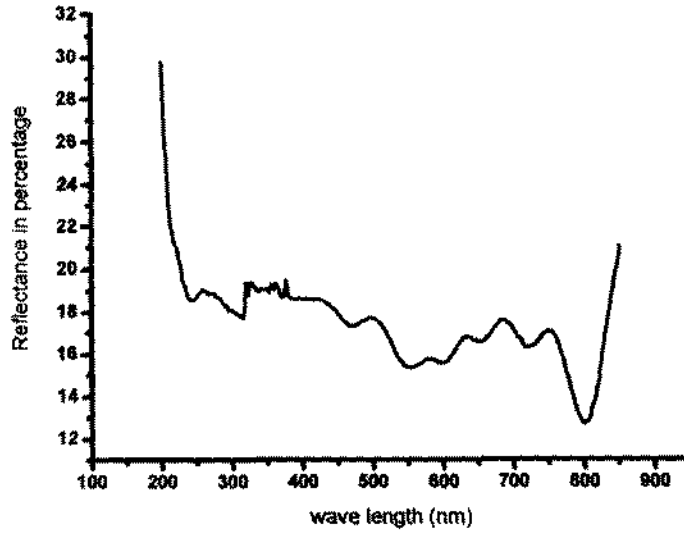


Figure 5.22 Graph of sample thickness 730nm and doping of copper 3.56% .

From the graph of sample 1 of thickness 240nm and doping concentration of copper (2.49%) it is clear that reflectance increase from 290 to 322nm i.e. in ultra violet (UV) spectrum and reach to the maximum at 840nm and after the high reflection was obtained. The pattern for the other samples were same, however slightly shifted toward highly wavelength.

Now to calculate the band gap energy of Cu (SnSbS) the following equation was used.

$$\alpha h\nu = A(h\nu - E_g)^n \quad 5.11$$

Here  $\alpha$  is the absorption coefficient,  $h\nu$  is the energy,  $A$  is the constant which depends on the transition probability  $E_g$  is the band gap energy and  $n$  is the number whose value for direct band gap is 2, for indirect band is 1/2, for direct forbidden transition is 2/3 and for indirect forbidden transition is 1/3. For calculating the  $E_g$ , we plotted a graph between energy  $h\nu$  along  $x$  - axis and  $(\alpha h\nu)^2$  along  $y$  - axis. The band gap of the films before and after doping was calculated by extrapolating the linear part of  $(\alpha h\nu)^2$  along  $y$ -axis and energy of photon ( $h\nu$ ) along  $x$ -axis for the curve to which  $(\alpha h\nu)^2 = 0$  (linear part of the vertical axis), which shows the semiconducting nature of the film.. Form the binding energies of different



concentration it is clear that the band gap energy decreases with the increasing of copper concentration.

**Table 5.7 Graph between copper concentration and Band gap energy**

S/no	Copper concentration (%)	Band gap energy(eV)
1	0	1.62
2	2.49	1.56
3	2.93	1.50
4	3.56	1.49

From the graph of band gap energy and doping percentage it is clear that by increasing doping of copper the band gap energy was decreased.

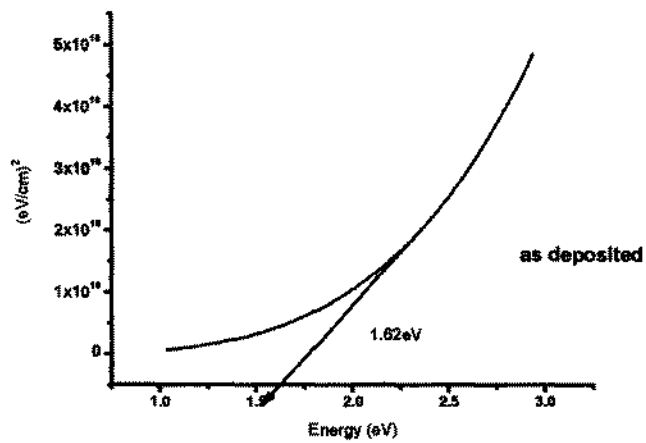


**Figure 5.23 Graph without doping**

The figure above shows the band gap energy of the film before doping which was 1.62eV.

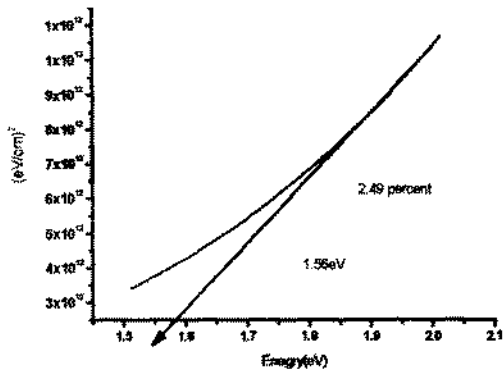


Figure 5.24 Band gap energy of sample 1, Of thickness 240nm and copper concentration 2.49%.

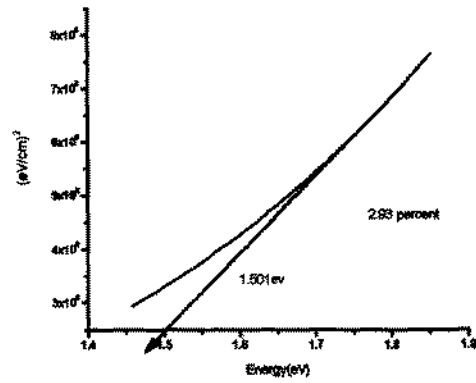


Figure 5.25 Band gap energy of sample no 2, of thickness 690nm and Copper concentration of 2.93%.

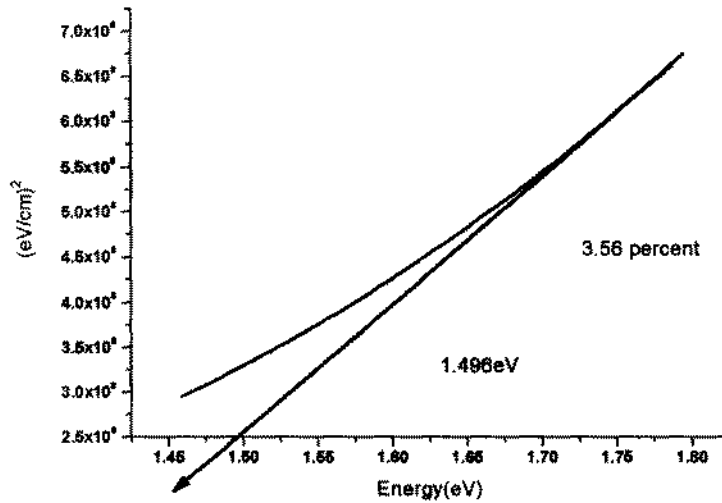


Figure 5.26 Graph of Band gap for 3.56%.

Band gap energy graph of sample '3' copper concentration 3.56% and 730 nm thickness

If a graph is plot between the copper concentration and band gap energy then it will show clearly that by increasing the concentration of copper the band gape energy decreases continuously as shown.

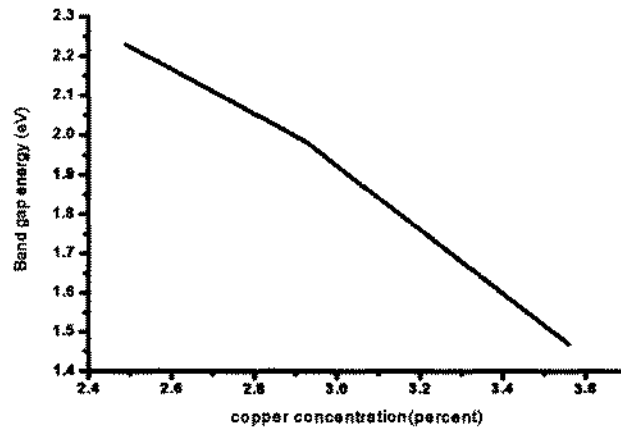


Figure 5.27 Graph of Copper (%) and Band gap energy.

From the graph it is clear that by increasing doping percentage of copper the Band gap energy of the thin films decreases.

## Conclusion

Tin Antimony Sulfide (SnSbS) thin films of various thicknesses were deposited on glass substrate by using two source thermal evaporation method, and the following conclusion were obtained. The optical spectra show that the absorption lines of the samples was shifted toward the shorter wavelength on increasing copper concentration. The interference pattern of the spectra reflects high smoothness of the samples. The band gap energy of the as-deposited and annealed samples were calculated by Tauc's formula by plotting a graphs between the linear portion of the  $(\alpha h\nu)^2$  and energy ( $h\nu$ ). It was confirmed that a significant changes occurred in the band gap energy of the films i.e. the band gap energy decreased from 1.62 to 1.49 eV. The optical properties helped to calculate the refractive index, dislocation density and micro strain of the films. However the grain sizes of the films were increased from 11.5 to 38.8 nm with copper concentration. The absorption coefficient was increased due to the decrease in the band gap energy. Also the thicknesses of the films were calculated from optical spectra and found in a complete agreement to the RBS measurements. The electrical properties of the films were analyzed with the help of Hall Effect measurement system. This showed that by increasing thickness and doping concentration of copper the conductivity and mobility of the films increased, while the resistance/resistivity of the films were decreased. The work was carried out with the intension to search for the cheap environmental friendly materials for solar cell. The doping was carried out to get a reduced resistivity thin film, by not compromising on the optical properties. It has been shown that copper doped Tin Antimony Sulfide may provide some better solution in solar cell technology.

## References

- [1] Poortmans, thin film solar cell fabrication, characterization and applications, Wiley series, U.S.A.2006
- [2] SreeHarsh, "Principles of physical Vapor Deposition. ,First edition, Elsevier, 2006.
- [3] Galvanic corrosion. Doctor. <http://www. Corrosion-doctors-org/forms-galvanic /galvanic corrosion.htm>. Retrieved on 29 April, 2011.
- [4]Thin film and Ink Tec awarded ID Tech Ex' Technical Development Manufacturing Award IDT Tech Ex, April 15<sup>th</sup> 2009
- [5]Christian Baran Rusu, J. Applied surface science 211, 1411, 2003.
- [6] Functional Polymer films Eds.r.Advincula and W.Knoll-Willey, 2011, ISBN.. 978-3527321902.
- [7] I.Kralova, J. Sjoblom, Biofuuele-renewable energy sources: Journal of Dispersion science and technology 31(3), 409 (2010).
- [8]Peter Gevorkien (1 August 2007). Sustainable energy systems engineering: the complete green building design resources. McGrew- hill professional .pp. 489 ISBN 978-0-07-147359-0 Retrieved 29 (Feb 2012).
- [9] A. Demribas, Recent advance in biomass conversion technologies. Energy Educational Science and Technology 6, 19 (2000).
- [10] Rathore NS, Panar NL. Renewable energy sources for sustainable development. New Dehli, India: New India publishing Agency(2007).
- [11] Okoro OI, Maduenme TC. Solar energy : A necessary investment in developing economy. International Journal of Sustainable Energy 25(1), 23 (2006)
- [12] "April 25, 1954: Bell Labs Demonstrates the First Practical Silicon Solar Cell". *APS News*(American Physical Society) 18 (4). April 2009.
- [13] Tsokos, K. A. (28 January 2010). *Physics for the IB Diploma Full Colour*. Cambridge University Press. ISBN 978-0-521-13821-5.

- [14] Phillip A. Laplante (2005). *Comprehensive dictionary of electrical engineering* (2nd ed.). CRC Press. ISBN 978-0-8493-3086-5
- [15] Datasheets of the market leaders: *First Solar* for thin film, *Suntech* and *SunPower* for crystalline silicon
- [16] Triple-Junction Terrestrial Concentrator Solar Cells. . Retrieved on 3 January 2012
- [17] B.G. Yacobi, *Semiconductor Materials: An Introduction to Basic Principles*, Springer 2003 ISBN 0306473615, pp. 1–3
- [18] Moss, S. J. and Ledwith, A. (1987). *The Chemistry of the Semiconductor Industry*. Springer. ISBN 0-216-92005-1.
- [19] K. Petkov, R. Todorov, D. Kozhuharova, L. Tichy, E. Cernoskova, P. J. S. Ewen. Changes in the physicochemical and optical properties of chalcogenide thin films from the system As-S and As-S-Tl. *J. Mat. Sci.* 2004; **39**:96–8.
- [20] E. Marquez, A. M. Bernal-Oliva, J. M. Gonzales-Leal, R. Pietro-Alcon, T. Wagner. Optical properties and structure of amorphous  $(As_{0.33}S_{0.67})_{100-x}Te_x$  and  $GexSb_{40-x}Sx_0$  chalcogenide semiconducting alloy films deposited by vacuum thermal evaporation. *J. Phys. D: Appl. Phys.* 2006; **39**:1793–7.
- [21] Cached, Corts, Froment, J. *Thin solid film*, Vol. 84, Page 361-362, 2000.
- [22] Rointan, *Handbook of deposition technologies for thin films and coatings*, second addition, noyes publications, New Jersey U.S.A.
- [23] Q. Lu, H. Zeng, Z. Wang, X. Cao, L. Zhang. Design of  $Sb_2S_3$  nanorod-bundles: imperfect oriented attachment. *Nanotechnology* 2006; 17:2098-7.
- [24] Z.S. El Mandouh, S.N Salama. Some physical properties of evaporated thin films of antimony trisulfide. *J. Mat. Sci.* 1990; **25**:1715-4
- [25] F. Aousgi, M. Kanzari. Study of the optical properties of the amorphous  $Sb_2S_3$  thin films *journal of optoelectronics and Advanced Materials* 2010; **12**:227-6
- [26] M. T. S. Nair, Y. Pena. J. Campos, V.M Garica, P.K. Nair. Cheminform Abstract: Chemically Deposited  $Sb_2S_3$  and  $Sb_2S_3-CuS$  thin films. *Electrochem. Soc.* 1998; 145:2113-8
- [27] Al Ghamdi, A. A. Optical band gap and optical constant in amorphous  $Se_{96-x}Te_4Ag_x$  thin Vacuum, 2006, 80(5), 400-405.

- [28] Bindu, K; Capos, J; Nair, M .T .S ; Sanchez, A ;Nair , P .K ,Semiconducting AgSbSe<sub>2</sub>; thin film and its application in a photovoltaic structure, *Semicond. Sci. Technol.*, 2005, 20 ,496-504.
- [29] Caricate, A, p; De Sario, M; Fernandez, M; Leggieri, G; Luches, A; Martino, M; Montagna, M; Prudenzano, F; Jha, A., chalcogenide glass thin film waveguides deposited by excimer laser ablation .*Appl.Surf Sci.* 2003, 208 -209(0), 632-637.
- [30] Kryukova, G.N ;Heuer, M; Wagner, G; Doering, T ; Bente K. Ssynthetic Cu<sub>0.507(5)</sub>Pb<sub>73(9)</sub>Sb<sub>8.15(8)</sub>11.6s<sub>20.0(2)</sub> nanowires. *J. Solid state chem.*,2005, 178(1),376-381
- [31] Mondouh, Z.S ;Salama, S, N., Some Physical properties of the evaporated thin films of antimony trisulfid. *J Mater, sci.* 1990, 25(3). 1715-1718.
- [32].Parenteau, M .M; Carlone ,C; Influence of temperature and pressure on thermo electronic transitions in SnS and SnSe semiconductors *Phys, Rev.*, 1990 B4(1),5227-5237.
- [33] Salem, A. M; Soliman Selim, M., Structure and optical properties of chemically deposited Sb<sub>2</sub>S<sub>3</sub> thin films, *J. Phys. D: appl. Phys*, 2001, 34, 12-17.
- [34] Chen, H; Zhu, C; Gan, F, preparation and optical properties of Sb<sub>2</sub>S<sub>3</sub> Microcrystallite. Silica Glassis by the solgel process. *J. Sol-Gel-Sci, Techn*, 1998, 12(3), 181-184.
- [35]. Karlova j. sjoblom, Biofuels renewable energy energy sources:a review. *Journal of Dispersion science and Technology* 31(13), 409(2010). IN refrance 7
- [36]Peter Gevorkien (1 August 2007). *Sustainable energy systems engineering: the complete green building design resources*. McGrew- hill professional .pp. 489 ISBN 978-0-07-147359-0 Retrieved 29 (February 2012).
- [37]A Demirbas ,Recent advances in biomass conversion technologies.*Energy Educatoinal science and Technology* 6, 19 (2007)
- [38]M. Y.Versavel, J.A. Haber: *Thin solid Films* 515,5767 (2007).
- [39]D.Bnnet, P.Meyers, *J. Mater, Res.* 13, 2740 (2007).
- [40]B.A Anderson, *Prog.Photovoltic. Res Appl.* 8,61 (2000)
- [41]A Gassoumi ,M Kanazari,*J.Optoelectornic.Adv. Mater.* 11(4), 414 (2009).
- [42]H.Dittrich, A. Stalder, D. Topa ,H.J Schimper, A. Basch, *Phys. Status Solidi A* 206(5), 1034(2009).
- [43]Shuey, R. T.(1975) *semiconducting oar minerals*, 415 P, Elesvier, Amsterdam.
- [44] Vaughan , D. J. and Craig , J .R. (1978) *Mineral chemistry of metal sulfides*, 493 P. Cambridge university press, Cambridge, U. K.

- [45] Vaughan, D.J (1985) Spectroscopy and chemical bonding in the opaque minerals. In F.J .Berry and D.J. Vaughan, Eds., Chemical bonding and spectroscopy in mineral chemistry, P. 251-292. Chapman and Hall, London.
- [46]Massalski, T. B; Okamoto, H; Kacprzak, L; Subramanian, P.R, Binary ALLOY Phase Diagrams. American society for metals: 1990
- [47]Krishna Seshan “Hand book of thin film”, deposition process and principles of physical vapor techniques 2<sup>nd</sup> addition.
- [48]Tips of electron Beam Evaporation by Midwest Tungsten Services. S.A , 2004
- [49]Ohring, Milton, Materials Science of Thin Films. Academic Press. P. 215.
- [50]cho,AY.Arther,J.R; jr (1975.”Molecular beam epitaxy.”.prog. Solid state chem. 10:157-192 doi:10.1016/00079-67 86(75)90005-9
- [51]Mishra and Ghosh, Preparation and structural characterization of ZnSe thin film by X-R-D technique, Indian J.Physics. 69A 261,1993
- [52]J.cheng ,v.k lazarav , et al .J .of vacuum science and Technology B , 27 , 148 (2009)
- [53]Crystal technology Trading Gmb H, Low pressure chemical vapour Deposition – Technology and equipment.
- [54]Elements of X-ray diffraction , 2<sup>nd</sup> Ed, by B.D cullity, Addison – Wesley, 1978 ( covers most techniques used in traditional material characterization)
- [55]Krishna Seshan “Hand book of thin film”, deposition process and principles of physical vapor techniques 2<sup>nd</sup> addition. ”
- [56] Griffiths, P.; de Hasseth, J.A. (18 May 2007). *Fourier Transform Infrared Spectrometry* (2nd Ed.). Wiley-Blackwell. ISBN 0-471-19404-2.
- [57][http://en .wikipedia . org /wiki/Fourier\\_infrared\\_specroscopy](http://en.wikipedia.org/wiki/Fourier_infrared_specroscopy).
- [58] Rhodes, R. (1995). *The Making of the Atomic Bomb*. Simon and Schuster. ISBN 978-0-684-81378-3.
- [59]Edwin Hall (1879). "On a New Action of the Magnet on Electric Currents". *American Journal of Mathematics* (American Journal of Mathematics, Vol. 2, No. 3) **2** (3): 287–92. doi:10.2307/2369245.JSTOR 2369245. Retrieved 2008-02-28.
- [60] Bridgeman, P. W. (1939). *Biographical Memoir of Edwin Herbert Hall*. National Academy of Sciences. .
- [61] "The Hall Effect". NIST. Retrieved 2008-02-28



- [62] Skoog, et al. Principles of Instrumental Analysis. 6th ed. Thomson Brooks/Cole. 2007, 349-351
- [63] Mehta, A. Deviations of Beer Lambert Law
- [64] Massalaski, T. B; Okamoto, H; Kacprzak, L; Subramanian, P. R, Binary Alloy phase Diagrams. American society for metals; 1990.
- [65] P. Smith, J. Parise, Acta Cryst. B, 41, 84 (1985)
- [66] Martin, P. M, "Handbook of deposition technologies for films and coating science, technology and applications," Elsevier, 3<sup>rd</sup> Ed, 2010.
- [67] P. Hanrahan and W. Krueger (1993), *Reflection from layered surfaces due to subsurface scattering*, in SIGGRAPH '93 Proceedings, J. T. Kajiya, Ed., vol. 27, pp. 165–174.
- [68] H. W. Jensen et al. (2001), *A practical model for subsurface light transport*, in 'Proceedings of ACM SIGGRAPH 2001', pp. 511–518
- [69] P. Kuleka and F. Munk, Z. Phys., 12 (1931) 593.
- [70]. "Elements of X-ray Diffraction", B. D. Cullity, Addison-Wesley Pub. Co., (1978).
- [71] P. P. K. Smith, Paris, Acta Crystallogr, B 41 (1985) 84-87.
- [72] Nath S. S., Chakdar D., and Gope G.; Synthesis of CdS and ZnS quantum dots and their applications in electronics, Nanotrends- A journal of nanotechnology and its application, 02(03), (2007).
- [73]. Nath S. S., Chakdar D., Gope G., and Avasthi D. K.; Effect of 100 MeV Nickel Ions on Silica Coated ZnS Quantum Dot, Journal of Nanoelectronics and Optoelectronics, 3, 1-4 (2008).
- [74]. R. Das, S. S. Nath, D. Chakdar, G. Gope and R. Bhattacharjee ; Preparation of Silver Nanoparticles and Their Characterization , Journal of nanotechnology online, (DOI : 10.2240/azojono0129)
- [75]. B. D. Hall, D. Zanchet and D. Ugarte ; Estimating nanoparticle size from diffraction measurements , Journal of Applied Crystallography, Volume 33, Part 6 (December 2000)
- [76] Bragg, W. L. *The Crystalline State: Volume I*. New York: The Macmillan Company, 1934.

[77]McQuarrie. Donald A. *Physical Chemistry: A molecular Approach*. Sausalito: University Science Books. 1997

[78] Shah, N.A. and W. Mahmood, 2013. Physical properties of sublimated zinc telluride thin films for solar cell applications. *Thin Solid Films*, 544:307-312.

[79] Shah, N., R. Sagar, W. Mahmood and W.Syed, 2012. Cu- doping effects on the physical properties of cadmium sulfide thin films. *Journal of Alloys and Compounds*, 512(1):185-189.

[80] Shah, N., A .Nazir, W. syed, S. Butt, Z.Ali and A.Maqsood, 2012. Physical properties and characterization of Ag doped CdS thin films. *Journal of Alloys and Compounds*, 512(1):27-32.

## Turnitin Originality Report

Thesis by Sabir Khan

From Thesis (No repository)

- Processed on 26-Feb-2015 17:02 PKT
- ID: 509922903
- Word Count: 9335

Similarity Index

6%

Similarity by Source

Internet Sources:

3%

Publications:

4%

Student Papers:

2%

**sources:**

1

&lt; 1% match (publications)

[Birgin, E.G., "Estimation of optical parameters of very thin films", Applied Numerical Mathematics, 200311](#)

2

&lt; 1% match (publications)

[Li, E., "Material parameters of InGaAsP and InAlGaAs systems for use in quantum well structures at low and room temperatures", Physica E: Low-dimensional Systems and Nanostructures, 200003](#)

3

&lt; 1% match (publications)

["Rutherford Backscattering Spectroscopy", Atomic and Nuclear Analytical Methods, 2006](#)

4

&lt; 1% match (student papers from 20-Jan-2014)

[Submitted to Higher Education Commission Pakistan on 2014-01-20](#)

5

&lt; 1% match (Internet from 08-May-2014)

[http://ethesis.nitrkl.ac.in/2914/1/THESIS\\_Asima\\_Print\\_07\\_06\\_2011.pdf](http://ethesis.nitrkl.ac.in/2914/1/THESIS_Asima_Print_07_06_2011.pdf)

6

&lt; 1% match (Internet from 26-Aug-2014)

[http://www.db-thueringen.de/servlets/DerivateServlet/Derivate-29144/Diss/Diss\\_Pub.pdf](http://www.db-thueringen.de/servlets/DerivateServlet/Derivate-29144/Diss/Diss_Pub.pdf)

7

&lt; 1% match (student papers from 22-Sep-2006)

[Submitted to University of Alabama, Huntsville on 2006-09-22](#)

8

&lt; 1% match (publications)